On the Evolution and Future Development of Electrodermal Diagnostic Instruments

by

William A. Tiller

Department of Materials Science and Engineering
Stanford University, Stanford, CA 94305

INTRODUCTION

Expenditure on health services in the U.S. is currently at the rate of well over $1 billion per day. As a percentage of gross national product (GNP), medical care expenditures have risen from 5% in 1960 to 10.5% in 1984. Because of this, in recent years government officials have predicted that the present rate of escalating costs will bankrupt the Medicare system by 1990. Many difficult health policy decisions obviously lie ahead and it is clear that fundamental reform of the U.S. health care system, and not just a minor adjustment of its parts, must become a national priority.

Within this context, I would like to propose that electrodermal diagnosis of human body systems holds the promise of being a much faster, much cheaper and perhaps a more accurate early method of body diagnosis than the present chemical analytic methods. Of course, at the moment, much research needs to be carried out to provide the mapping transforms between the electrical signatures determined by electrodermal measurements and the chemical patterns associated with various medical syndromes or

health pathologies.

At this point one might well ask, "What do I mean by electrodermal diagnostic measurements?" In response, I would say that this involves placing electrodes at various locations on the skin of the body, applying a fixed voltage or electrical current between electrode pairs for a specific amount of time and recording the response of the body to this stimulus in the form of a current or voltage, respectively, as a function of time. Analysis of these response magnitudes and patterns is thought to be directly related to the state of function of the various organs and body systems. Electrodermal studies of human skin have been carried out since the turn of the century with the view to learning more about the body's electrical characteristics and patterns of function, and some of this early work culminated in the invention of the ECG, EEG and EMG technologies, important "linchpins" in modern medical technology.

From one vantage point, the body can be looked at as a complex interconnected electrical power generation, power distribution and power use system much like that found in a modern state or province. Thus, the circuit theory concepts of electrical engineering are relevant here. One imagines a type of internal "wiring" into which organs feed a variety of current and out of which other body systems act as electrical loads and draw current. The energy streams from a number of organs appear to flow into one of the many internal conducting channels and appear to flow either to or "through" a set of surface points. It is the degree and character of energy flow that is correlated with the functioning

condition of that set of organs, and that degree of energy flow is thought to generate the difference in electrical conductance between these special surface points and the surrounding tissue. Thus, these points become information access windows to the functioning state of specific organ and body systems.

From a larger perspective, every molecule, cell, tissue wall, muscle fiber, organ or body system are electromagnetic oscillators having some complex frequency pattern. Thus, they are radiators of electromagnetic energy over a broad frequency spectrum with the radiant frequency range for a specific body part being lower, the larger is the size of the part. From this viewpoint, the body functions as a multi-element antenna array which gives rise to both a near-field standing wave pattern of electromagnetic energy (the mathematically imaginary component of the radiation), plus a far-field traveling wave pattern of the electromagnetic energy (the mathematically real component of the radiation). Within both patterns, information exists concerning organ and other body system functioning; however, it is much easier to access this information via the near-field pattern.

In the not too distant future, one can expect instruments to appear which probe the information patterns of this near-field electromagnetic "aura" of a human for diagnostic purposes. However, at present, our device technology is limited to body surface mapping of this information and the present paper focuses specifically on the electrical information available at the skin's surface.

From what may be called by some a "more enlightened"

perspective, the physical body can be looked at as a four-dimensional space-time instrument of a higher dimensional consciousness, also that the physical body is coupled to other bodies that function in more subtle realms of nature. If so, then the substance of these other bodies will also radiate patterns of energy of a subtle type in much the same fashion as the electromagnetic substance of the physical body. Thus, in the more far distant future, one can also anticipate the availability of devices for monitoring these patterns of subtle information and for diagnosing the condition of the various subtle bodies. The point to be made here is that the electrical devices being developed today to monitor the electrical information available in, on and around the physical body serve as a kind of "metaphor" for future work at more subtle levels of human functioning. Now, let us return to the more conventional perspective.

In this paper, I wish to trace the modern development of electrodermal instruments so that we will have a better understanding of its origins. Unfortunately, this sketchy historical review cannot be complete partially because many of the instruments in use have little written documentation, nor have they been written up in the professional literature. The available information can be divided into two domains of electrodermal studies involving either macro or micro size electrodes. The large electrode (diameter $\geq$ 1 cm) results, which became the background terrain for modern galvanic skin response (GSR) studies, were well defined by the work of Rosendal, which was carried out prior to World War II and published during the early 40's [1]. The small

electrode (diameter ≤ 0.1 cm) results, beginning in the late 40's, revealed an interesting heterogeneity to the electrical properties of skin on living mammals.

In part, with small electrodes, one discerns an array of high electrical conductivity points patterned over the body that can be discriminated to lie along a number of discrete high conductivity lines. Although no histological difference can be discerned at present between a high conductance point region and the adjacent tissue, it has been shown that a direct correlation exists between (a) the difference in electrical conductance at the point versus the surrounding skin and (b) the hypnogogic state of the individual; i.e., waking, sleeping, depressed, elated, hypnotized, etc. Thus, they are, at least in part, neurally influenced.

LARGE ELECTRODE STUDIES

The skin consists of two main layers, an outer thin layer called the epidermis and a thick inner layer called the dermis. The outermost 0.001 to 0.01 cm of the epidermis is called the stratum corneum, which consists of flattened dead cells and constitutes a large contribution to the electrical impedance of the skin. Although somewhat squashed, the stratum corneum cells still contain electrolyte, are separated from each other by narrow channels of electrolyte and are cation (+ve ion) permeable. The moisture content of the inner layers of cells in the stratum corneum is much higher than that of the outer layers so that moisture steadily percolates from the inner to the outer layers

depending upon the external humidity. The electrical impedance of the stratum corneum is primarily capacitive in nature but is short- circuited by resistive channels between the cells. Its capacitance arises from the 10-100 layers of cells connected in parallel with the single cell capacitance arising from the polar nature of the two membrane layers plus the adjacent space charge in the interior cell medium.

The simplest electrical equivalent circuit for the case of zero applied voltage is that shown in Fig. 1. Here, C is the capci-tance of these layers of cells connected in parallel, R_2 is the short-circuiting resistance across the cells and $R_1 << R_2$ is the resistance of the deep tissues. If this was a true, fixed parameter, electric circuit, the application of a constant voltage V_o would lead to a current response, I(t), like that shown in Fig. 2 where

$$i_o = V_o/R_1 \qquad (1a)$$

$$i_\infty = V_o/(R_1 + R_2) \qquad (1b)$$

and

$$\tau = R_1R_2C/(R_1 + R_2) \cong R_1C \quad \text{for } R_1 << R_2 \qquad (1c)$$

Thus i_o relates to deep tissue effects while i_∞ relates to stratum corneum effects.

Rosendal [1] showed that, when a negative DC surface voltage is applied such that a steady current is moved outwards through the skin (cathodal current), the D.C. resistance falls, as

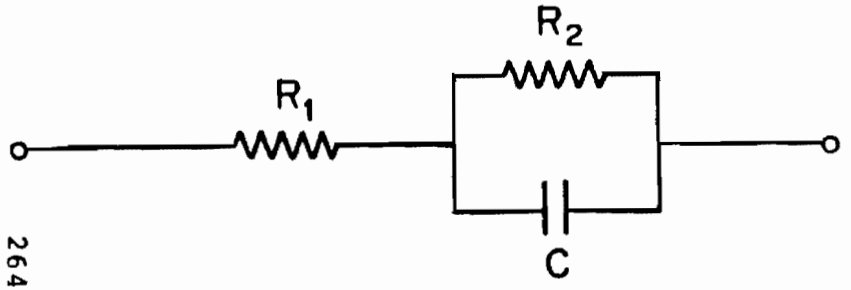

1. The simplest frequency independent electrical equivalent circuit used for skin measurements.

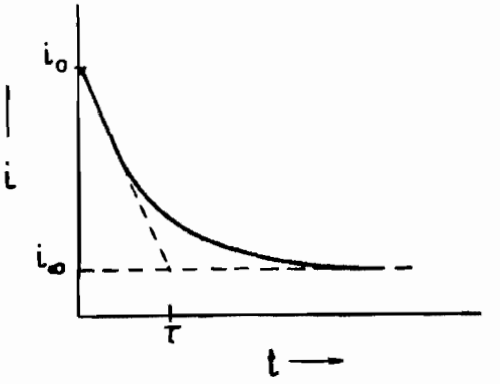

2. Current waveform arising from the application of a constant DC voltage to the circuit of Fig. 1.

shown in Fig. 3, and vice versa for current moving inwards through the skin (anodal current). The ratio of the two saturation levels of resistance can be as large as 10:1 and the time constant for the process is many seconds long. When the applied voltage is AC at ~ 1000 Hz, the impedance slowly increases with time, but to a smaller degree than shown in Fig. 3. Such an effect is attributed to the selective permeability nature of the cell membranes (they pass +ve ions more easily than -ve ions) and the short-circuit channels between the cells. At very high frequencies, this effect will be absent because there is insufficient time in a half cycle for ion transport between the cell boundaries, and the current passes instead through the body of the cells. Thus, a frequency dependent resistance is expected at low frequencies.

Rosendal also found that moistening the stratum corneum with electrolyte revealed a marked decrease of DC resistance that became constant in about 30 minutes at a value 5 to 10 times lower than the initial value. This indicates electrolyte enhancement in the stratum corneum by a diffusion process just as occurred with cathodal current flow. When a voltage between 2 and 4 volts was applied after this constant resistance had been reached, a further decrease in resistance was noted so that the resistance approached that of the internal epidermal tissue. This decrease of resistance at $V_o > 2$ volts was accompanied by a marked feeling of tingling in the skin which became stronger with increasing voltage and which is due to electrolyte dissociation of the water molecules in the stratum corneum and the ultimate generation of H_2 gas at very high dissociation levels.

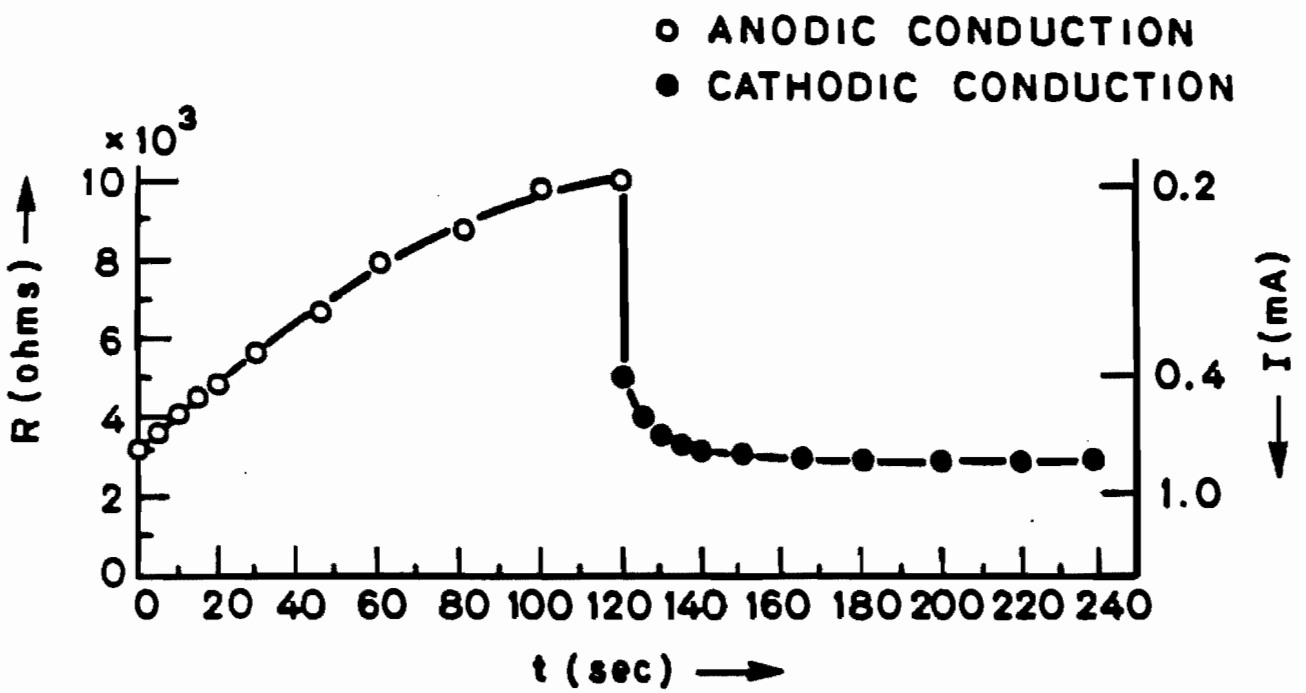

3. Time dependence of the electrical resistance, R, of the skin for a 2 volt applied DC potential (7 cm_2 of skin moistened for 20 min with saturated KCl solution). (Courtesy of T. Rosendal)

Assuming the equivalent circuit model of Fig. 1, Lykken [2] applied 100 m sec voltage pulses of V_o = 0.5 volts to the skin and studied the relative contributions of the various skin layers to the parameters in Fig. 1. By abrading the skin, he found that C was reduced to undetectable values and that $R_1 + R_2$ was reduced by 2/3. Therefore, the capacitance resides in the stratum corneum for this long time-constant process (see Fig. 3), while the major resistance is fairly evenly divided between the stratum corneum and the deeper epidermal tissue. He also found that, for voltages above 2V, the resistance was nonlinear with voltage and continued to decrease as the voltage was increased.

Swanson and Webster [3] obtained similar findings to Lykken by progressively scraping away layers of the stratum corneum and found that the electrical equivalent circuit model of Fig. 4a gave good match to the experimental data when they gave specific values to the circuit parameters. Gatzke [4] used the model of Fig. 4b and showed that, especially if Ag/AgCl electrodes are used, the electrode parameters are insignificant and the model reduces to that of Fig. 4c which is essentially Lykken's [2] model except for the addi-tion of interface ($V_m(i)$) and skin (V_S) potentials. He found the electrolyte characteristics to be quite important; with a high con-centration (5-10%) NaCl electrolyte, the typical resistance values will decay by a factor of 25 in about one hour; with a low concentration (0.5%) NaCl electrolyte, very little resistance decline was noted with time.

Nagel and Tiller [5] found via a frequency-dependent study wherein the real and imaginary parts of the skin impedance were

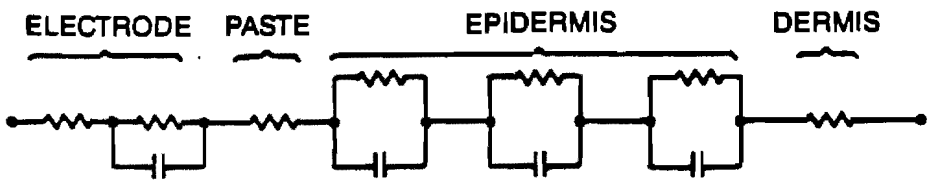

(a)

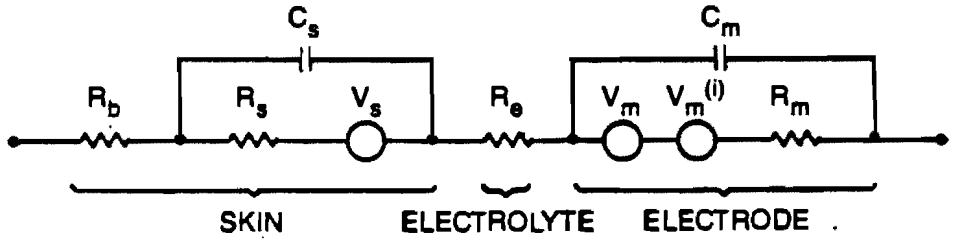

(b)

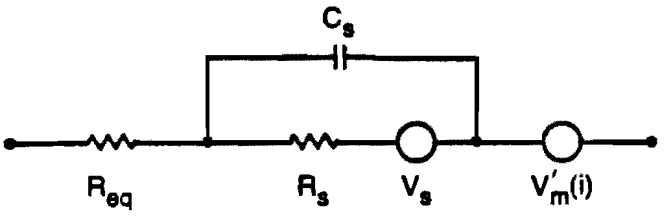

(c)

4. (a) Form of the electrical equivalent circuit of the skin and electrode system which matches the experimental data without assuming frequency dependent parameters.

   (b) Alternate systems viewpoint circuit.

   (c) Important circuit elements after neglect of the electrodes.

plotted (Cole-Cole plots), that skin exhibits both a high frequency (τ_I ~ 1-10 μsec) and a low frequency (τ_{II} ~ 10-100 sec) electrical equivalent circuit in series (See Fig. 5), with the Z_I and Z_{II} parameters in Fig. 5 being diffusional admittances which are functions of frequency [see Appendix B for details].

In a study of electrocutaneous stimulation, Kume and Ohzu [6] used bipolar constant voltage pulse trains with ring type electrodes located on the forearm and observed the response of the high frequency circuit as illustrated in Fig. 6. We note that τ_I ~ 5 μsec in this case.

The studies of Lykken [2], Swanson and Webster [3] and Gatzke [4] all relate to the low frequency circuit (τ_{II}), where the diffusional admittance is primarily related to ion transport processes through the membrane. For the high frequency circuit, electrical dipole oscillations of the membrane fixed charge sites are expected to be responsible for τ_I.

Schimmel [7] appears to be one of the first to develop a medical diagnostic instrument based upon this large electrode information. In the Schimmel Segment Electrogram, the body is divided into horizontal sections and a pair of electrodes is placed in each section on the anterior surface, as indicated in Fig. 7. Each electrode pair is stimulated with a sequence of: (1) a 13 Hz negative voltage sawtooth impulse of 18 second duration, (2) a similar positive-going wave and, finally, (3) a 26 second quiescent period at zero volts. The current is recorded during each of the three phases and indicated in Fig. 7b. Schimmel indicates that diagnostic information is implicit in the

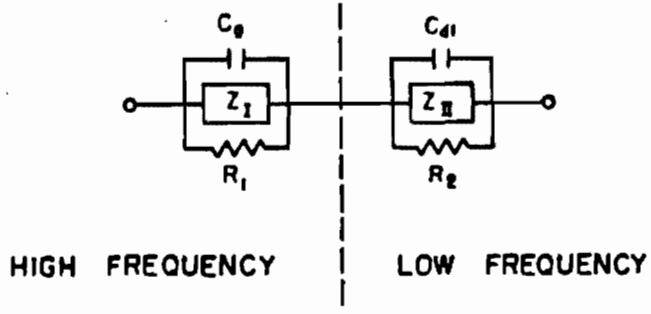

5. Electrical equivalent circuit generated from skin measurements using AC conductance techniques and complex plane analysis.

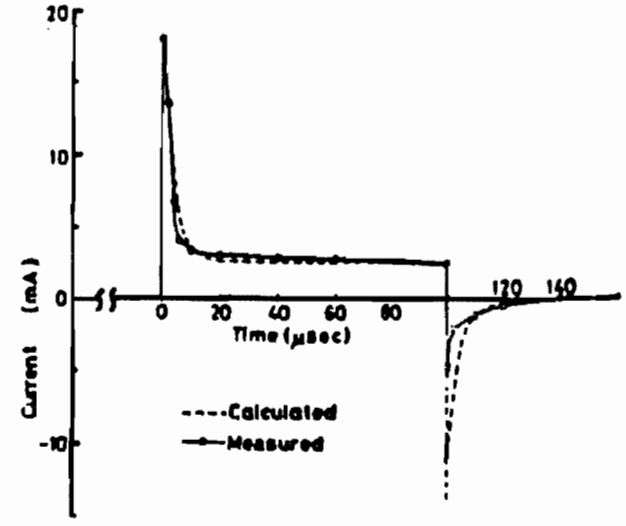

6. Stimulus current corresponding to a constant voltage pulse applied to the skin through a concentric electrode.

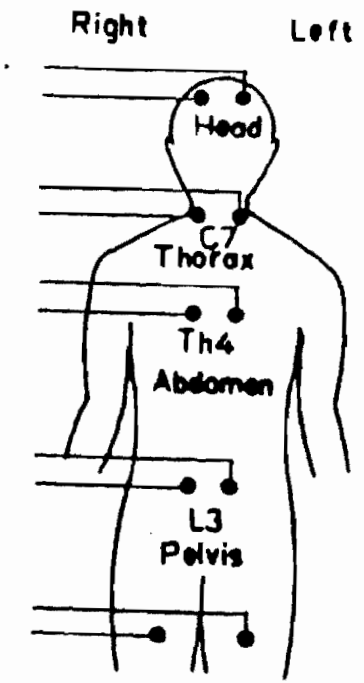

7. (a) Body placement of electrodes in the Segment Electrograph technique.

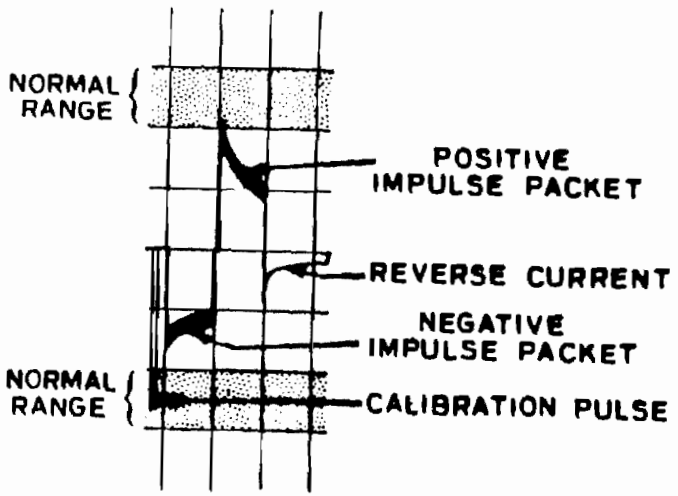

7. (b) Illustration of electrical pulse cycle on recording paper.

following features: (1) the magnitude of the current pulse in the stimulation phase can fall in either (a) the normal region, (b) above the normal region (hyperfunc-tion) or below the normal region (subfunction); (2) the shape of the current trace in the stimulation phase and (3) the magnitude and shape of the response current phase. The normal shape of the current trace in the stimulation phase is a slightly curved trace at about 35 degrees to the horizontal with drop in amplitude and clear cut border line (see Fig. 8a). The subfunctioning energy condition is illustrated by a shortening or almost total absence of current amplitude and a transformation of the sloping shape towards a rectangular shape (see Fig. 8b). This is interpreted by Schimmel as increased energy rigidity combined with decreased energy flow. The hyper-functioning energy condition is indicated by increased current amplitude and an increase in trace angle above 35 degrees (see Fig. 8c). This is interpreted as an indication of rising energy flow, of increasing degree of inflammation and of oxidation. Similar interpretations are also given to the features of the response current waveform (see Fig. 9).

From the basic information given earlier [1-6], we note that this technique deals with the low frequency portion of the skin circuit and thus involves ion transport across selective permeability membranes. The driving voltage sees the sum of the resistances from the left and right electrodes so the generated current is cathodal from one and anodal from the other (see Fig. 2). The net resistance increases with time due to ion transport effects so the current trace in the stimulation phase decays with time, as noted in Fig. 8. The subnormal functioning condition is

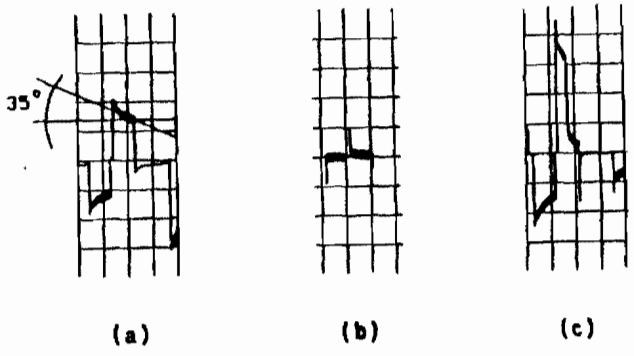

8. Illustration of the general types of current trace resulting from the stimulation voltage wave: (a) normal body function, (b) sub-normal body function and (c) hyper body function.

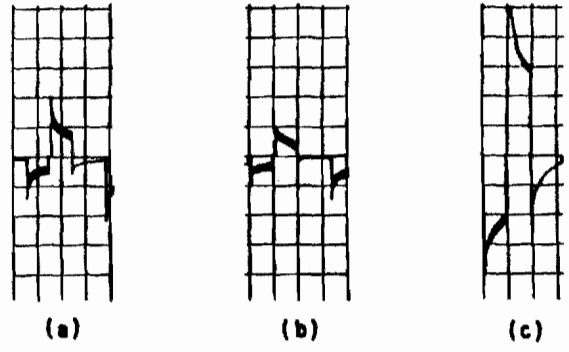

9. Illustration of the response current trace: (a) normal body function, (b) sub-normal body function and (c) hyper body function.

thus due to high skin impedance which comes from a combination of low electrolyte content and/or low tissue fluid content. The hyperfunctioning condition is thus due to low skin impedance which comes from a combination of high electrolyte content and/or high tissue fluid content.

The stimulation and response current waveforms can be predicted from first principles just as Fig. 2 and eqs. 1 apply to a constant applied voltage. The qualitative results for a positive impulse voltage and for a positive followed by a negative impulse voltage are given in Fig. 10. In each case, there is a calculated response current, as shown in Fig. 10 (b) and (c), depending upon R_1, R_2 and C of Fig. 1 and the periods t_1 and t_2 in Fig. 10.

From the foregoing, we see that the Schimmel technique measures the basic ion concentration, the mobility of these carriers and the permeability selective character of the cell membranes in the skin in various sectors of the body. The direct connection between these skin parameters and the body's state of health is not immediately obvious. However, the skin is one of the body's major waste disposal systems and it is a linkage medium to various nerve endings. It is reasonable to deduce that a shift of the skin conductance parameters from the normal range signals either a local waste disposal problem or a local neural problem connected to some organ or body system malfunction. Or it is possible that the local skin conductance parameters, all by themselves, indicate the state of local body health or pathology in ways we do not yet understand. Finally, it is possible that we are kidding ourselves and the local skin conductance parameter

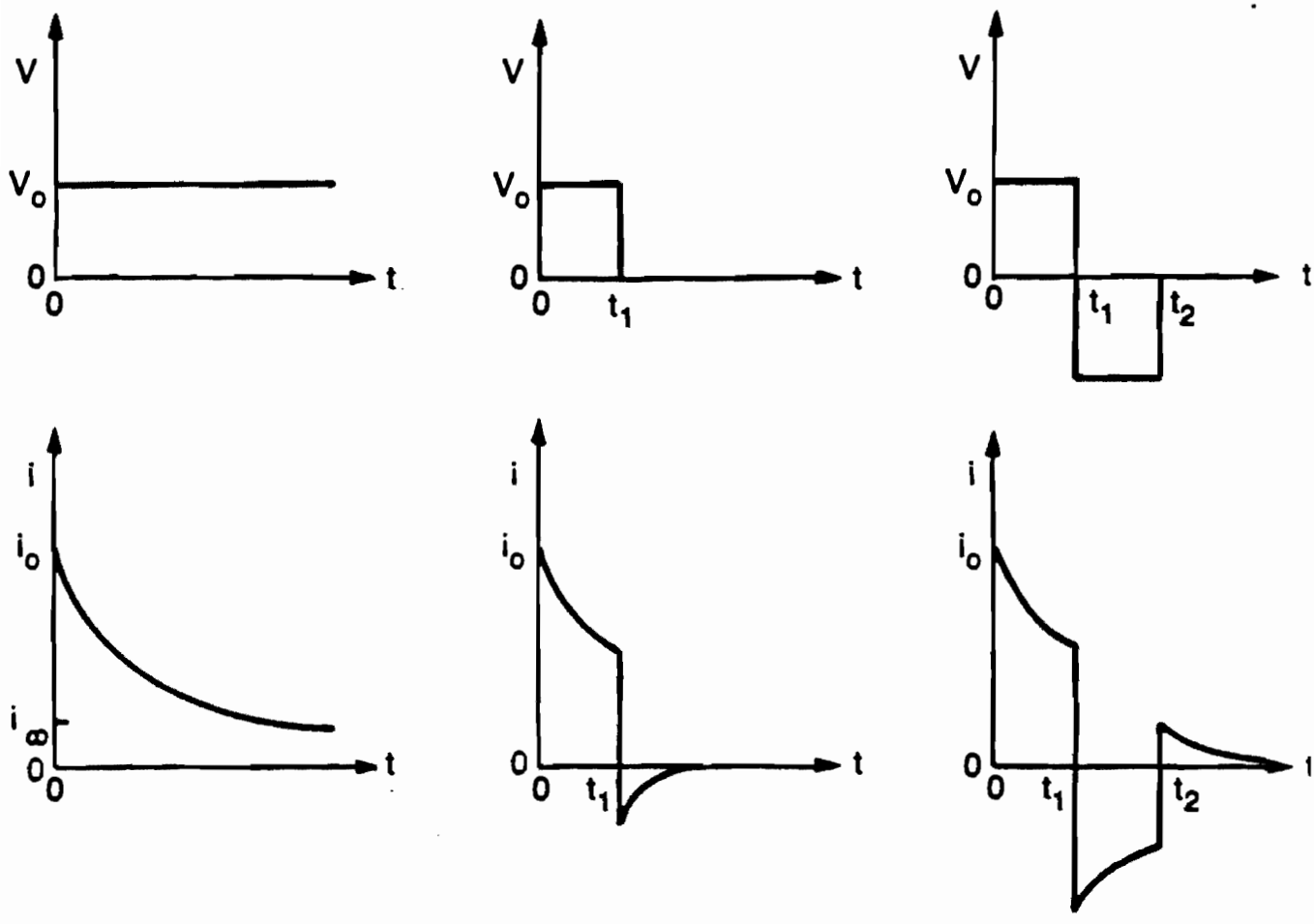

10. Response current waveforms to various voltage waveforms being applied to the circuit of Fig. 1.

values only indicate the local state of hydration, ion content and membrane permeability.

SMALL ELECTRODE STUDIES

In the early 1950's, Y. Nakatani [8] used a 12 volt DC source and passed current through the skin of a patient discovering, thereby, that some points had a much higher electrical conductance than the surrounding sites. He named these "good conductivity points" and linked them up with an imaginary line known as a "good conductivity line" (Ryodoraku). This became known as the "Ryodoraku" technique and the measurement device was called the "Neurometer." Here, the patient holds in his/her hand the mass electrode, and the good conductivity points are tested with the tip of a search electrode. Because of the large voltage used, this response current is largely due to electrolytic dissociation of H_2O. In Europe, Niboyet [9], Bratu [10] and Brunet [11] also studied the properties of these high conductivity points. In China, many similar studies were conducted [12-14]. They found that the location of these high conductivity points and lines coincided amazingly well with the points and meridians of Chinese classical acupuncture. Using a Nakatani neurometer, Matsumoto [15] showed that 80 percent of acupuncture points could be detected.

According to Nakatani [16], acupuncture points have a low resistance due to the fact that excitation of sympathetic nerves had caused enlargement and opening of the sweat and sebaceous

glands at these sites. However, others [14] failed to substantiate this proposal. Ishikawa [17] claimed that the high conductivity was due to reflex changes in subcutaneous blood vessels. However, Niboyet [18] found that acupuncture points on cadavers also had the characteristic of highest local conductivity. Others [14] substantiated this finding and Shenberger [19] demonstrated the high conductivity characteristic on a human subject in life, after death and after embalming.

In an attempt to quantify the conductance observations a little better, Reichmanis et al. [20] used a rolling-type probe in a 2 volt bridge circuit and found that conductance maxima could be found within a 1 cm^2 area surrounding the Large Intestine meridian on the forearms and that more prominent maxima were located at the acupuncture points. Wulfson [21] investigated 27 points and obtained an average resistance of 794 - 197 K ohms when bilaterally compared with control points 0.25 inches away from them. The average resistance of the control points was 1404 - 306 K ohms. Using a miniature array of 36 electrodes, Reichmanis et al. [22] were able to compare both acupuncture point and control point regions without the need to search for the local conductance maxima. Most of the points on the Lung and Triple Heater meridians were shown to be statistically different from the control point. Using a special ring electrode design, Hyvarinen and Karlsson [23] studied conductance maxima on the ear and found them to be a factor of 10-30 higher than the surrounding skin. Further, assuming a skin impedance model like Fig. 1, Reichmanis et al. [24] used Laplace transform techniques to evaluate R_1, R_2 and

C for points H_2 and H_4 of the Heart meridian relative to adjacent control points. They found R_1, R_2 and C to be about 3-6 times lower, 1.5 to 2.5 times lower and 1 to 2 times higher, respectively, for the acupuncture points.

All of the foregoing has dealt with electrical conductance properties of these special points and it is perhaps not surprising to learn that these points also have higher electrical potentials than the surrounding tissue [14,25]. Becker et al. [26] determined the skin electrical potential and found that some acupuncture points on the body showed positive electrical potential in contrast to surrounding areas. Brown et al. [27] reported that most of the high potential points were present bilaterally on the body and were in corresponding positions with those of classical acupuncture points. Dumitrescu et al. [28] reported that acupuncture points had electrical potentials 2-6 millivolts higher than that of the surrounding areas. Of course, this is just what one would exepect if the skin cell membranes were cation permeable and the acupuncture points had a higher conductivity via a higher electrolyte content. Diffusion of positive ions to the surface of the skin would be enhanced at the acupuncture points leading to the excess positive potential at these points.

Fraden and Gelman [29] and Fraden [30] used a constant current source to investigate nonlinear effects at acupuncture points. A bipolar current source was employed in order to pass a 10 μA square wave current at frequencies from zero to 1000 Hz through certain acupuncture points. The skin impedance was investigated and it was found to be larger when positive current flowed

(anodal) than when negative current flowed (cathodal) in accordance with the large electrode results of Fig. 2. This nonlinearity, defined as the ratio of positive impedance to negative impedance, is reduced as the frequency is increased above 1 Hz. The time constant for the resistance changes was found to be ~ 1-5 seconds for the positive polarity and ~ 0.5-3 seconds for the negative polarity. This is much shorter than τ_{II} in Fig. 2; however, here the current density is much higher. In fact, the current density is sufficiently high that the local voltage across the skin exceeds 2 volts so that H_2O dissociation is occurring at all times. They found that the skin impedance was suddenly reduced by 5-10 times when the negative current was applied for several seconds. This phenomenon, which has been called "point breakdown" is accompanied by a change of all point properties and is thought to be associated with the destruction of the cell membranes.

Besides the Nakatani neurometer [8], two major pieces of diagnostic equipment have been developed based upon the small electrode skin conductance findings and we shall now discuss these. No commercial diagnostic equipment has yet been developed which exploits the electrical potential properties of acupuncture points or which utilizes the constant current source technique.

In the low frequency domain, the Voll dermatron [31] has been the most popular instrument. Its predecessor was the K&F Diatherapuncteur unit which is no longer being manufactured; however, it forms the basis of all the other EAV (Voll instruments) and its functioning is described in Appendix A.

With the Voll dermatron, shown in Fig. 12, in the diagnostic mode, the A.P. is charged with - 8-10 μA at a DC voltage of - 1 volt. The method of doing this is via a ball electrode contacting the skin at an applied pressure of - 500-1400 psi, while a large cylindrical electrode is held in the patient's off-side hand to complete the electrical circuit. The meter on the instrument is designed to record the skin's electrical conductance rather than the electrical resistance. The scale of the meter has been adjusted so that a reading of 50 indicates "normal" while a reading of >50 is defined as indicating an irritated situation with the degree of irritation increasing as the reading increases. A reading of <50 is defined as a degenerative condition with the degree of degeneration increasing as the reading drops.

A second and perhaps more important diagnostic indicator is the indicator drop (I.D.); i.e., the reading decreases from its maximum initial value to a final value with time. As a rule, the I.D. occurs within 1 to 3 seconds. In a retarded I.D., suggestive of an incipient functional disturbance, the period is thought to depend upon the intensity and scope of the pathologic process in the organ being measured. The interval of the I.D. is usually 10-20 seconds when the initial measurement value is about 50; it is 20-30 seconds when the measurement value drops to 30 and it is greater than 30-60 seconds when the reading drops to 20 or less. This is basically the same type of behavior as noted earlier with the Schimmel device. Here, when the initial skin conductance is smaller (resistance higher), the anodal current flowing through the skin for fixed applied voltage is smaller so it takes longer

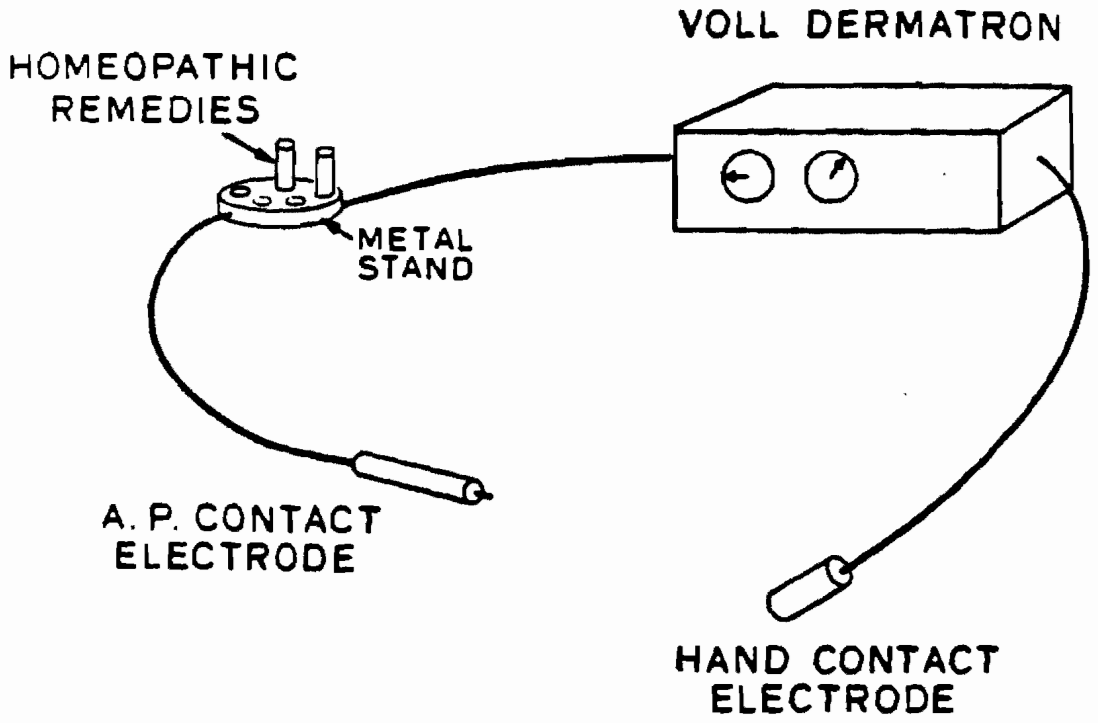

12. Schematic illustration of the Voll dermatron with electrodes.

for the ion transport to occur through the membrane walls. Thus, the resistance rises more slowly with time and the I.D. is slower. This device also measures skin conductance levels (combined electrolyte content and water content) and permeability selectivity of the membranes. Even for the same value of conductance, an increase of I.D. value by a factor of - 5-10 in a pathologic versus a healthy case indicates less permeability selectivity for the membranes involved. Once again, it is not readily seen how the electrical conductance and permeability selectivity values of the A.P.'s are directly connected to specific organ or body system functioning.

The Motoyama AMI instrument [32] applies a DC potential of 3 volts between a number of meridian terminal points and a large indifferent electrode on the wrist, as indicated in Fig. 13. It utilizes a skin electrical equivalent circuit like that shown in Fig. 1 and samples the very short time domain (high frequency domain). A current waveform like that shown in Fig. 2 is sampled by the instrument. He defines 4 parameters (supposedly independent) for describing this current response: (1) BP (before polarization), the current value before ionic polarization in the skin proceeds against the externally applied electric potential ($i(t = 0)$); (2) AP (after polarization), the current value which still flows even after the completion of this short time polarization ($i(t = 10^{-3}$ sec)); (3) IQ (integrated polarization charge), the total transferred electric charge of ions incurred during this short time polarization and (4) TC (time constant), the intercept point of the initial current slope with the AP level.

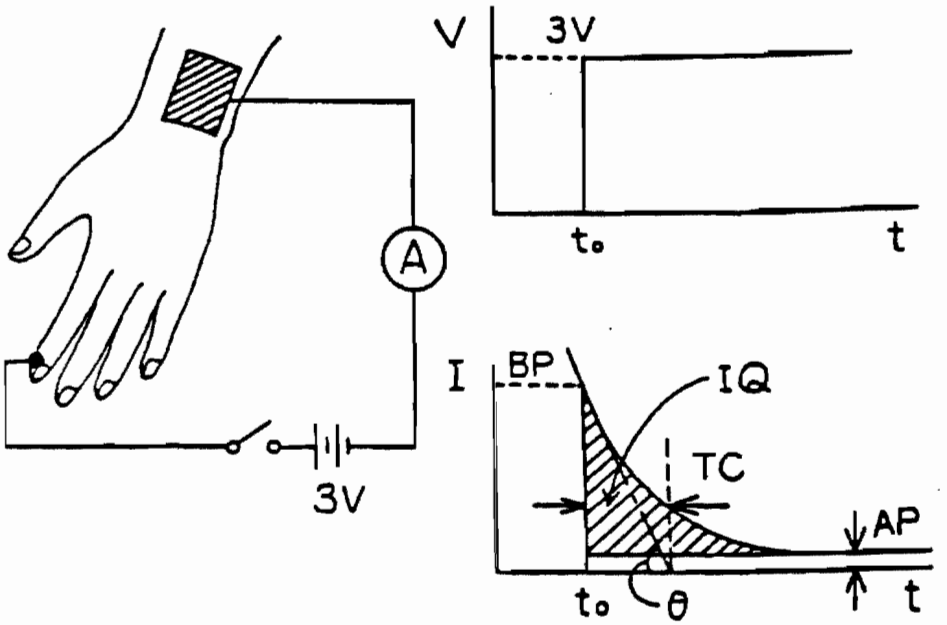

13. Single electrode arrangement in the Motoyama technique, applied voltage impulse and response current waveform for the system.

One should not confuse the current waveform and circuit parameters involved in Fig. 13 with the current waveform and circuit parameters involved in Fig. 3, because the time domains are completely different. If one could assume constant circuit parameters for both the low frequency (Fig. 3) circuit and the high frequency (Fig. 13) circuit, then the value of i from the high frequency circuit is approximately the value of i_o for the low frequency circuit. In analogy with eqs. 1, let us use primed values to denote the value of R_1, R_2 and C for the high frequency circuit and unprimed values for the low frequency circuit. Then, we have

$$BP = V_o / R' \tag{2a}$$

$$AP' = V_o / (R_1' + R_2' \tag{2b}$$

$$\tau_I = R_1' R_2' C' / (R_1' + R_2') \approx R_1' C' \quad \text{for } R_1' \ll R_2' \tag{2c}$$

$$i_o = AP' = V_o / R_1 = V_o / (R_1' + R_2') \tag{2d}$$

$$i_\infty = V_o / (R_1 + R_2) \tag{2e}$$

$$\tau_{II} = R_1 R_2 C / (R_1 + R_2) = R_1 C \quad \text{for } R_1 \ll R_2 \tag{2f}$$

If V_o < 2 volts, then the current is given as a function of time in the following way:

$$i(t) = V_o \{ A e^{-t/\tau_I} + B e^{-t/\tau_{II}} + C^* \} \quad (3a)$$

where

$$C^* = V_o / (R_1' + R_2' + R_2) \quad (3b)$$

$$B = V_o / (R_1' + R_2') \quad (3c)$$

and

$$A = V_o / R_1' \quad (3d)$$

Motoyama has shown [32] that the BP current travels primarily in the dermis with only a 30% influence coming from the epidermal layer. He has also shown that the seat of the C' capacitance involves charge transfer across the basal membrane barrier between the epidermis and dermis, as illustrated in Fig. 14. It is tempting to identify R_2 with the stratum corneum resistance, R_2' with the epidermis and R_1' with the dermis; however, there is no completely valid justification for this. In Fig. 15, log [ln (i-i)] is plotted versus log [time] to show these two processes on the same time scale for the $V_o < 2$ volt case where no electrolysis occurs and for the $V_o = 3$ and 4 volt cases where some electrolysis occurs. The current drops by about a factor of 20-50 over the first 10^{-4} seconds and by about another factor of 10 over the next 10^3 seconds. In actuality, we cannot use constant parameters for these low and high frequency circuits but must

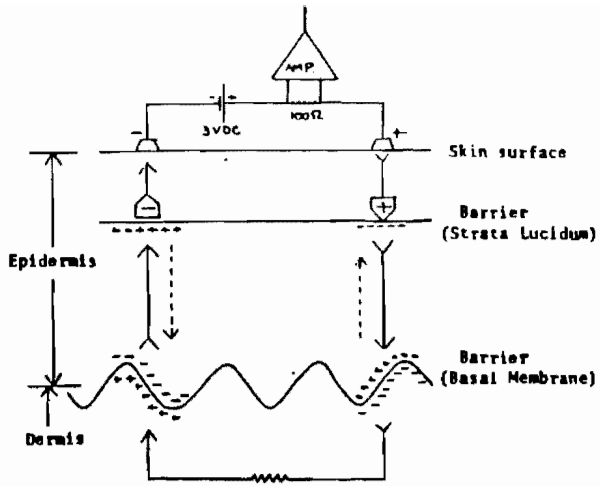

14. Generalized diagram of the ionic accumulations in the dermis and epidermis.

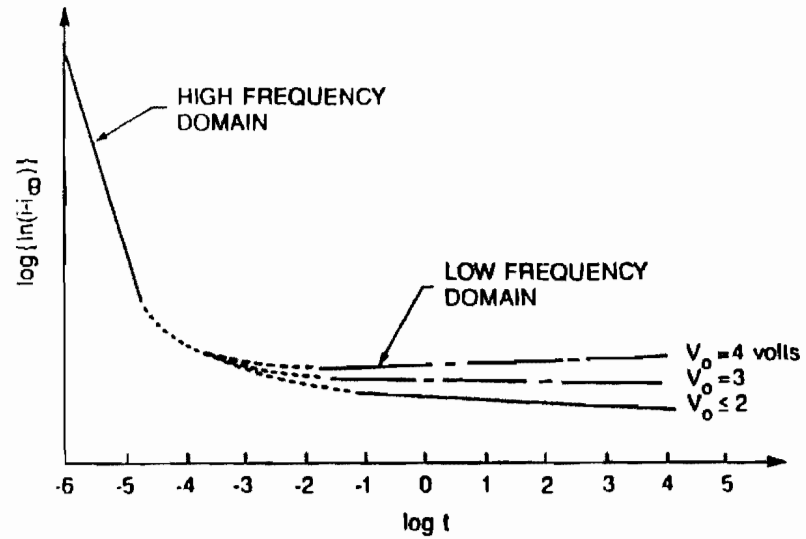

15. Schematic representation of the current vs. time plot over the entire time domain (9 decades).

use the approach of Fig. 5. If the parameters were constant in the high frequency circuit, the mathematics requires that $\alpha = 1$ in the following defining equation:

$$IQ = \frac{\alpha}{2} TC \left[BP - AP \right] \tag{4}$$

This author checked the data sheets for 30 patients studied via the AMI [37] and found that α was not unity but ranged from 0.3 to 0.5 to fit the data. Either the important circuit parameters are time varying in this small time domain or the AMI machine is not responding rapidly enough to accurately measure in the initial 10 secs, or both. Although the AMI utilizes a 1 MHz clock, this only guarantees accurate time sampling in 10 μsec blocks, not 1 μsec blocks. A 10 MHz clock would be needed to accurately sample the initial few μsecs.

Motoyama's technique is to attach electrodes to the distal points of all meridians on the hands and feet and measure each point in turn, à la Fig. 13, automatically with a computerized system. In the Chinese system of notation, the 12 Jing distal points indicated in Fig. 16 have been used for acupuncture point treatment for centuries and quantitatively by Akabane since 1952 [33,34], and more recently by Ionescu-Tirgoviste [35]. These points are thought to play an important role in the "six energy axes" [36], as illustrated in Fig. 17. In the Motoyama notation, these are called the Sei points and there are 14 of them, as indicated in Fig. 18. After the electrode placement stage, which may take ~ 20 minutes, the measurement stage of the 28 electrodes

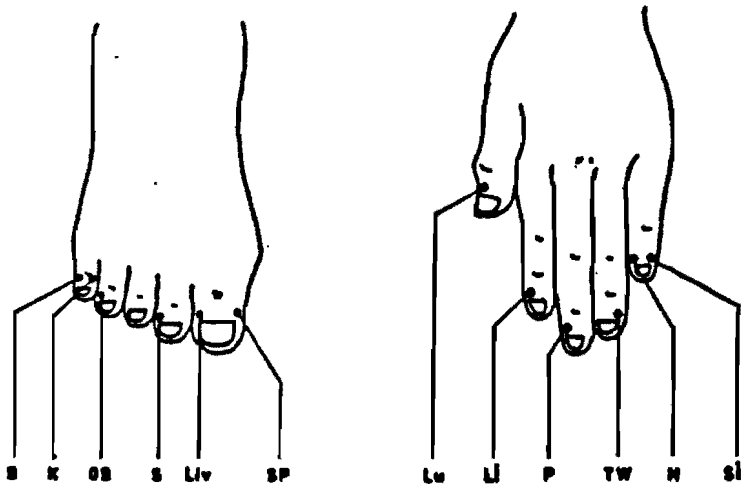

The location of Jing distal points.

16. The location of the 12 Jing distal points.

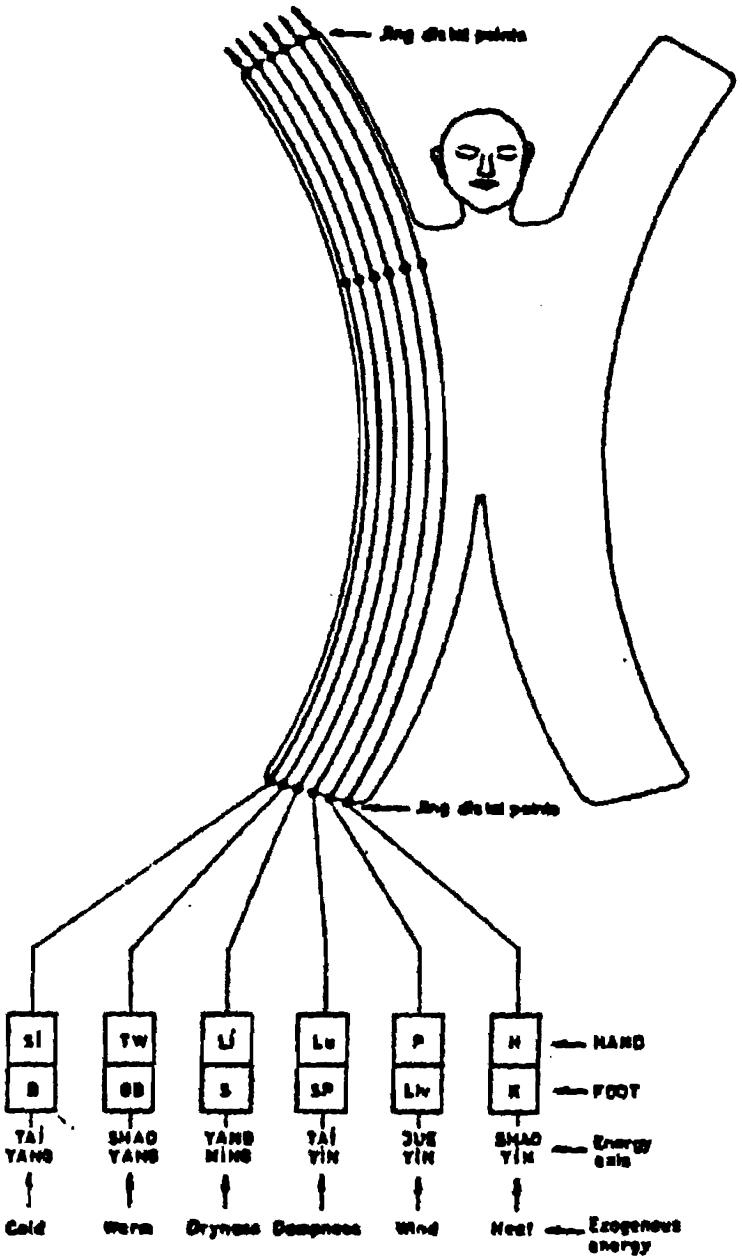

The Six Energy Axes

17. Schematic illustration of the six energy axes.

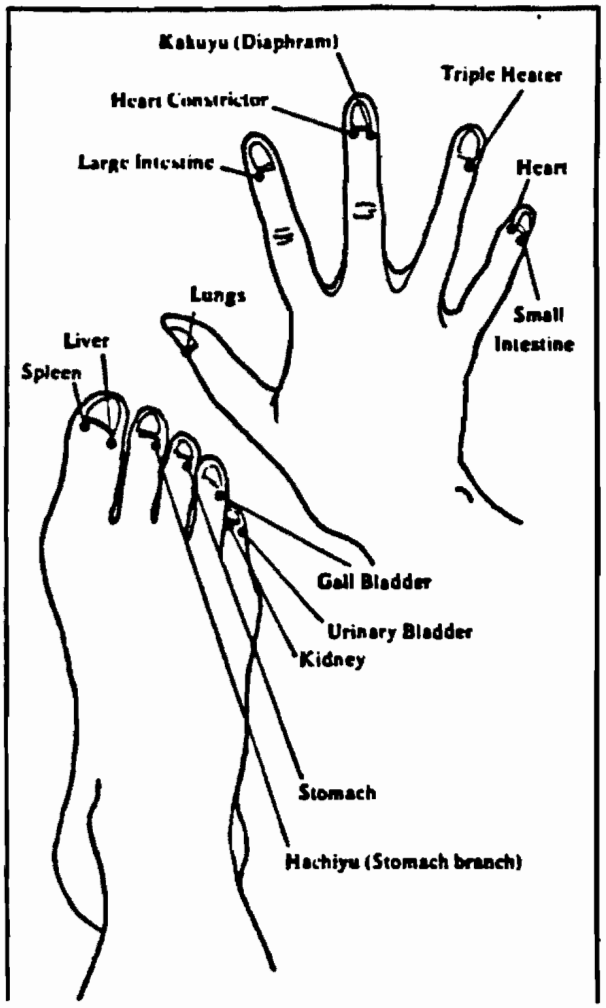

18. The location of the 14 Sei points.

begins. The automated measurement process of all the BP, AP, TC and IQ requires only a few minutes and the computer prints out these values for each of the points. The computer also prints out the standard deviations for each of these points and the changes between the left and right side values relative to the sum of the values for the 28 points. It also prints out the body averages, left-right differences on average, hand-feet differences on average and the average standard deviation. When the values fall outside of the expected range for a healthy person, they are "flagged" for the viewer. In a general sense, values that are too high are interpreted to mean that the body is in an excited state--often signalling the beginning of disease. Values that are too low are interpreted to mean that the whole autonomic nervous function is reduced generally through a chronic disease.

In a more specific vein, the following are average values in adults for the Phoenix area [37].

$$\begin{aligned} BP_{Avg} &= 1600\text{-}2000 \\ AP_{Avg} &= 20\text{-}30 \\ TC_{Avg} &= 8.5\text{-}12 \\ IQ_{Avg} &= 3500\text{-}4000 \end{aligned} \tag{5}$$

If the patient's IQ value is high, it is thought to indicate congestion or blockage and the higher it is, the more toxic is the

condition. When the value is low, a weakness is thought to exist in the whole reaction of the individual. When the TC is high, the individual is thought to be armored, stressed, chronic tightness; if it is low, the indication is weakness, apathy, given up. If the AP is high, this is thought to indicate an overstressed sympathetic nervous system (sweaty palms, tight individual); if it is low, the indication is for weak defenses and poor recoverability (meditators fall here, but this is normal for them). Finally, if the BP is high (> 2100), the indications are for a mildly toxic to a very ill condition (depends on the IQ value), perhaps an allergy; if low (<1600), the individual is weak in overall energy and complains of severe fatigue [37].

Reflecting on both the Voll and the Motoyama devices, the measurements appear to reflect classical resistance and capacitance values and no direct electrical connection yet appears to specific inner organs or body system. The field is in great need of such connection delineation.

Before leaving this section, it is important to note a major difference between these two techniques that has not yet been brought to light. In the Motoyama technique the electrodes may be attached by a nurse and the data gathered in the automatic mode to be examined by the doctor later; i.e., the doctor need not be present when the data is gathered. In the Voll technique and any other hand-held electrode technique, the doctor is in the psychic loop "patient/machine/practitioner" and can unconsciously influence the readings by subtle tilts of the electrodes, subtle changes in pressure, etc. Thus, it may begin to be used uncon-

sciously in a radiesthetic mode. This is an important factor that needs to be carefully studied before electrodermal devices become a commonplace tool for the health practitioner.

As a final point for this section, one must also account for any device-induced distortion of the body current signal. A discussion of this topic is given in Appendix C.

SOME CONNECTIONS

Rosenblatt [38] attempted to investigate (1) changes in functioning of an internal organ (heart rate) correlations with selected acupuncture points which are related to the internal organ, (2) changes in functioning of that organ correlations with acupuncture points that are unrelated to the organ even though these points will be in close anatomical proximity to a point that is related to the organ function, and (3) correlations in skin conductance changes at a selected acupuncture point versus an unrelated A.P. with the functioning of an internal organ (heart rate).

Rosenblatt [38] found that when subjects attempted to alter their heart rate via biofeedback using a tone generator, there was a significant correlation ($P = 0.01$) with changes in the skin conductance at a preselected heart meridian A.P. (both for raising and lowering the heart rate). The conductance increased as the heart rate increased. No corresponding correlations were found at other A.P.'s or in localized areas of skin near but not on the selected A.P.'s. Conversely, when the subjects used biofeedback to change the conductance of a preselected heart point

(H-7), there was a significant correlation in the actual change in heart rate. Using points unrelated to heart functions, as the conductance was changed, no corresponding changes occurred in the heart rate. This is a very important result and it will be very valuable to obtain similar checks with the functioning criteria of other organs.

EARLY WARNING CANCER DETECTION

Kobayashi [39] used a Nakatani neurometer and found simultaneous abnormalities in the bilateral readings of 6 specific meridians identified as the "signature of cancer." These were the pericardium, heart, triple heater, spleen-pancreas, kidney and gall bladder meridians. He divides cancer into 7 stages by weight: cancer-free, microgram (μ), small milligram (M^1), large milligram (M^2) and gram level or clinical cancer (early gram, G^1, median gram, G^2, and terminal gram, G^3). He observed a statistically signficiant difference between the μgram cancer and the non-cancer groups ($P < 0.001$). He also found a significant difference between the M^1-level cancer and the non-cancer groups ($P < 0.1$). In general, he felt his electrodermal signature to be an effective early warning system for cancer detection.

SUMMARY DEDUCTIONS FROM THE DATA

Aside from conductivity effects (electrolyte concentration and ion mobility) and permeable membrane selectivity effects, which are all localized to the epidermis/dermis region, the one

special feature that is unaccounted for is the battery-like effect of the A.P.'s; i.e., they will supply current to a high impedance load. Another special feature is the enhanced positive potential of several millivolts at the A.P. skin compared to surrounding skin. If one just evaluated the surface potential based on simple diffusion of + ions from the inside of the cell to the surface, the potential would be only - several microvolts. Thus, for it to be as large as millivolts requires a driving field pushing the + ions out onto the skin.

If a magnetic vector potential field, A, flowed along the meridians, an electric field, E, would exist given by

$$\vec{E} = -\nabla \phi - \frac{\partial \vec{A}}{\partial t} . \qquad (6)$$

This additional negative field at the surface of the skin would require a larger transfer of positive ions and a correspondingly larger surface potential, ϕ, such as has been measured. The induced field indicates that this is probably the source of the battery-like effect observed at the A.P.'s and points to an internal body source which may be the organs. Interestingly enough, this same time-varying $\vec{A}$ field gives rise to a microwave EM field passing out through the A.P.'s and this field could dissociate membrane-bound water molecules in the stratum corneum tissue to give the A.P.'s their enhanced electrical conductivity compared to the surrounding tissue. This seems to be the connection that we need to understand better than we presently do. It is perhaps this connection that will reveal the diagnostic efficacy of these

new devices that monitor the skin and predict the state of organ pathology. Much more study is needed to test this hypothesis; however, it seems clear that one should at least add a battery to the circuit of Fig. 1.

Considering an E-field directed outwards along a meridian to the surface in the stationary state, the electric force will cause the ions to pile up until the back-diffusion force exactly cancels the $\vec{A}$-generated $\vec{E}$-field. This moves positive ions outwards from the inner body to the dermis and epidermis regions so that the ionic conductivity of these regions experience a net increase of magnitude depending exponentially on the magnitude of the $\vec{E}$-field. This manifests itself in the magnitudes of R_1 and R_2 and probably also of C. Thus, by measuring the change in magnitude of these parameters with changes in the subject's health state, one is gaining a measure of the state of the internal organs via the $\vec{A}$-generated $\vec{E}$-field linkage.

CONCLUSIONS

1. There are several effective electrodermal techniques in present use and we understand both how they work as well as what they actually measure.

2. There does appear to be some beginning experimental support for, and a possible theoretical model to explain, connectivity between the organs and their specific A.P.'s.

3. There does appear to be important differences between the hand-held moving electrode modality of skin measurement and the

fixed, multiple electrode, automatic switching modality of skin measurement.

4. Although we are just at the beginning of this new technology, it is likely that new and more effective devices will appear during the next decade that could significantly reduce health care costs.

ACKNOWLEDGEMENTS

The author would like to thank Drs. Harvey Bigelson, Peter Madill and Roger Wicke for very helpful discussions.

REFERENCES

1. Rosendal, T., "Studies on the Conductivity Properties of Human Skin to Direct Current," Acta Physiol. Scand. 5, 130-151 (1943) and "Further Studies on the Conducting Properties of Human Skin to Direct and Alternating Current," Acta Physiol. Scand. 8, 183-202 (1944); 9, 39-49 (1945).
2. Lykken, D., "Square Wave Analysis of Skin Impedance," Psychophysiol. 7, 262-275 (1971).
3. Swanson, D. and Webster, J., "A Model for Skin-Electrode Impedance," in: Biomedical Electrode Technology, Eds: J. Hood and P. Purser (Academic Press, N.Y., 1974) pp 117-128.
4. Gatzke, R., "The Electrode, a Measurement Systems Viewpoint," ibid., pp 96-116.
5. Nagel, L. and Tiller, W. A., "Dielectric Response in Human Skin," unpublished.
6. Kume, Y. and Ohzu, H., "Electrocutaneous Stimulation for Information Transmission, I: Optimum Waveform Eliciting Stable Sensation Without Discomfort," Acupuncture and Electro-Therapeut. Res. Intl. J. 5, 57-81 (1980).
7. Schimmel, H. W., The Segment Electrogram (Vega, Grieshaber KG, Postfach 10, D-7622 Schiltock (Schwarzwald).
8. Nakatani, Y., "An Aspect of the Study of Ryodoraku," Clinic of Chinese Medicine 3, 54 (1956); "Skin Electric Resistance and Ryodoraku," J. Autonomic Nerve 6, 52 (1956).
9. Niboyet, J. E. H., "Nouvelle Constatations sur les Proprietes Electriques des Points Chinois," Bull. Soc. Acup. 30, 7 (1958).

10. Bratu, I., "The Value of Electrical Skin Resistance in Acupuncture," Communic. Dtsche. Ztschr. Akupunk 6, 11 (1960).

11. Brunet, R., "Introduction a l'Etude de l'Acupuncture," Bull. Soc. Acup. 37, 7 (1960).

12. Zhang Xiehe et al., " The Principle of Diagnosis and the Method of Application of Meridian Detector," Journal of the Institute of Traditional Chinese Medicine 9, 579 (1958).

13. Zeng Zhaolin et al., "A Study on the Determination of the Normal Value of Cutaneous Conductance and Temperature of Acupuncture Points," Journal of Traditional Chinese Medicine and Pharmacology of Shanghai 12, 33-37 (1958).

14. Zhu Zong-Xiang, "Research Advances in the Electrical Specificity of Meridians and Acupuncture Points," Am. J. Acupuncture 9, 203-216 (1981).

15. Matsumoto, T., Acupuncture for Physicians (Charles C. Thomas, Springfield, Illinois, 1974).

16. Manaka, Y., "Ryodoraku and Clinic," Gynecology and Obstetrics 32(12), 893 (1978).

17. Sekigawatachio, Journal of Kanazawa Juren Medical Society 63, 182 (1959).

18. Niboyet, J. E. H. et al., "Comptes Rendu de Recherches Experimentales sur les Meridiens. Chez le Vivant et Chez le Cadavre," Actes de Illiemes Journees Internationales d' Acupuncture, 47-51 (1958).

19. Shenberger, R. M., "Acupuncture Meridians Retain Identity After Death," Am. J. Acupuncture 5, 357-361 (1977).

20. Reichmanis, M., Marino, A. and Becker, R., "Electrical Correlates of Acupuncture Points," IEEE Trans. Biomed. Eng. 22, 533-535 (1975).

21. Wulfson,N., Yoo, J. and Gelineau, J., "Twenty-seven Acupuncture Points and Their Electrical Resistance," in Handbook of Medical Acupuncture, Ed: F. Warren (Van Nostrand, New York, 1976).

22. Reichmanis, M., Marino, A. and Becker, R., "DC Skin Conductance Variation at Acupuncture Loci," Am. J. Chinese Med. 4, 69-72 (1976).

23. Hyvarinen, J. and Karlsson, M., "Low Resistance Skin Points that May Coincide with Acupuncture Loci," Med. Biol. 55, 88-94 (1977).

24. Reichmanis, M., Marino, A. and Becker, R., "Laplace Plane Analysis of Impedance Between Acupuncture Points H-3 and H-4," Comp. Med. East and West 5, 223-229, 285-297 (1977).

25. Podshibiaky, A. K., "Variations of Electrical Potential with Respect to Internal Organs and their Relation to 'Active Points' of the Skin," J. Physiology USSR 44, 357 (1955).

26. Becker, R. D. et al., "Electrophysiological Correlates of Acupuncture Points and Meridians," Psychoenergetic Systems 1, 105 (1976).

27. Brown, M., Ulett, G. and Stern, J. "Acupuncture Loci: Techniques for Location," Am. J. Chinese Med. 2, 67-74 (1974).

28. Dumitrescu, I. F. et al., "Contribution to the Electrophysiology of the Active Points," International Acupuncture Conference (Bucharest), 20, 1977.

29. Fraden, J. and Gelman, S., "Investigation of Nonlinear Effects in Surface Electroacupuncture," Am. J. Acupuncture 7, 21-30 (1979).

30. Fraden, J., "Active Acupuncture Point Impedance and Potential Measurements," Am. J. Acupuncture 7, 137-144 (1979).

31. Voll, R., "Twenty Years of Electroacupuncture Diagnosis in Germany, A Progress Report," Am. J. Acupuncture 3, 7-17 (1975).

32. Motoyama H., How to Measure and Diagnose the Functions of Meridians (Intl. Assoc. for Religious Psychology, 1975), and "Electrophysiological and Preliminary Biochemical Studies of Skin Properties in Relation to the Acupuncture Meridian," Intl. Assoc. for Religion and Parapsychology 6, 1-36 (1980).

33. Kajdos, V., "The Akabane Method as Applied to Acupuncture," Am. J. Acupuncture 2, 266 (1974).

34. Dale, R. A., "A New Three-Phase Acupuncture Law," Am. J. Acupuncture 10, 325 (1982).

35. Ionescu-Tirgoviste, C., Bajenaru, O., Zugranescu, D. et al., "Electric Skin Potential of the Jing Distal Points in Diabetics With and Without Clinical Neuropathy," Communic. USSM, Bucharest, 1983.

36. Ionescu-Tirgoviste, C. and Bajenaru, O., "Electric Diagnosis in Acupuncture," Am. J. Acupuncture 12, 229-238 (1984).

37. Bigelson, H., (M.D.), Phoenix, AZ, private communication.

38. Rosenblatt, S. L., "The Electrodermal Characteristics of Acupuncture Points," Am. J. of Acupuncture 10, 131-137 (1982).

39. Kobayashi, T., "Early Diagnosis of Microcancer by Cancer Check of Related Acupuncture Meridians," Am. J. of Acupuncture 13, 63-68 (1985).

40. Warburg, E., " Ueber das Verhalten sogenannter unpolisirbarer Electroden gegen Wechselstrom, Annelen der Physik und Chemie 67, 493-499 (1899).

41. Fricke, H., "The Theory of Electrolytic Polarization," The Philosophical Magazine 14, 310-318 (1932)

42. Grahame, D. C., "Mathematical Theory of the Faradaic Admittance," J. of the Electrochemical Society 99, 370c-385c (1952).

43. MacDonald, J. R., "Simplified Impedance/Frequency-Response Results for Intrinsically Conducting Solids and Liquids," J. of Chemical Physics 61, 3977-3996 (1974).

44. Geddes, L. A. and Baker, L. E., "Optimum Electrolytic Chloriding of Silver Electrodes," Medical and Biological Engineering 7, 49-56 (1969).

45. Edelberg, R., "Electrical Properties of the Skin," in Biophysical Properties of the Skin, Ed: H. R. Elden (Wiley-Interscience, New York, 1971).

46. Venables, P. H. and Martin, I., "Skin Resistance and Skin Potential," in A Manual of Psychophysiological Methods, Eds: P. H. Venables and I. Martin (John Wiley & Sons, New York, 1967) pp 53-102.

47. Schwan, H. P., "Determination of Biological Impedance," in Physical Techniques in Biological Research, Ed: W. L. Nastuk (Academic Press, New York, 1963) pp 323-407.

48. Cole, K. S. Membranes, Ions and Impulses (University of California Press, Berkeley, 1968).

49. Cole, K. S. "Electric Phase Angle of Cell Membranes," J. of General Physiology 15, 641-649 (1932).

50. Cole, K. S. and Cole, R. H., "Dispersion and Absorption in Dielectrics, I: a.c. Characteristics," J. of Chemical Physics 9, 341-351 (1941).

51. Schwan, H. P., "Biological Impedance Determinations," J. of Cellular and Comparative Physiology 66 (Suppl. 2), 5-11 (1966).

52. Schwan, H. P. "Electrode Polarization Impedance and Measurements in Biological Materials," Annals of the New York Academy of Science 148, 191-209 (1968).

53. Yokota, T. and Fujimori, B., "Impedance Change of the Skin During the Galvanic Skin Reflex," Japanese Journal of Physiology 12, 200-209 (1962).

54. Yamamoto, T. and Yamamoto, Y., "Electrical Properties of the Epidermal Stratum Corneum," Medical and Biological Engrg. 14, 151-158 (1976-a).

55. Barnett, A., "The Phase Angle of Normal Human Skin," J. of Physiology 93, 349-366 (1938).

56. Tregear, R. T., "Physical Functions of the Skin," in Theoretical and Experimental Biology (Academic Press, London, 1966), vol. 5.

57. Yamamoto, T. and Yamamoto, Y., "Dielectric Constant and Resistance of Epidermal Stratum Corneum," Medical and Biological Engrg. 14, 494-499 (1976-b).

58. Lawler, J. C., Davis, M. J. and Griffith, E. C., "Electrical Characteristics of the Skin," J. of Investigative Dermatology 34, 301-308 (1960).

59. Burton, C. E., David. R. M., Portnoy, W. M. and Akers, L. A., "The Application of Bode Analysis to Skin Impedance," Psychophysiology 11, 517-525 (1974).

60. Teorell, T., "Application of 'Square-Wave Analysis' to Bioelectric Studies," Acta Physiologica Scaninavica 12, 235-254 (1946).

61. Sandifer, J. R. and Buck, R. P., "An Algorithm for Simulation of Transient and Alternating Current Electrical Properties of Conducting Membranes, Junctions and One-Dimensional, Finite Galvanic Cells," The J. of Physical Chemistry 79, 384-392 (1975).

62. Yoganathan, A. P., Gupta, R. and Corcoran, W. H., "Fast Fourier Transform in the Analysis of Biomedical Data," Medical and Biological Engrg. 14, 239-244 (1976).

APPENDIX A

The K+F Diatherapuncture Functional Description

The circuit diagram for the diagnostic part is given in Fig. 11 where we note that it consists primarily of a vacuum tube voltmeter with the anode current being displayed on a meter. The measuring voltage, applied to the patient via the small diameter electrode pressed strongly against an A.P., ranges between 0.135 and 2.070 volts and the current passing through the body ranges between 11.25 μA and 5.5 μA for a resistance change from 12 KΩ to 380 KΩ. The calibration curve for this instrument is also shown in Fig. 11.

The measurement instrument shows an indicator deviation of 50 (50% of full scale) as long as the A.P. and the corresponding organ are free from pathologic disturbances. If, instead of the human body, either a resistance of 95 KΩ or a voltage of 0.87 volts is connected between the two electrodes, the indicator deviation becomes 50. In addition, if a galvanometer of high ohmic resistance is connected to one hand-electrode and one stylis-electrode, a much higher reading is obtained from an A.P. than from a random skin point. Thus, although an A.P. must certainly be thought of as having an electrical impedance, it appears to act as a type of battery as well.

When the electrodes of Fig. 11 are applied to the body, the following sequence of events happens: (1) The skin resistance is placed in parallel with the cathode-grid resistance, Rg, set to produce a strong negative bias at the grid electrode. (2) This

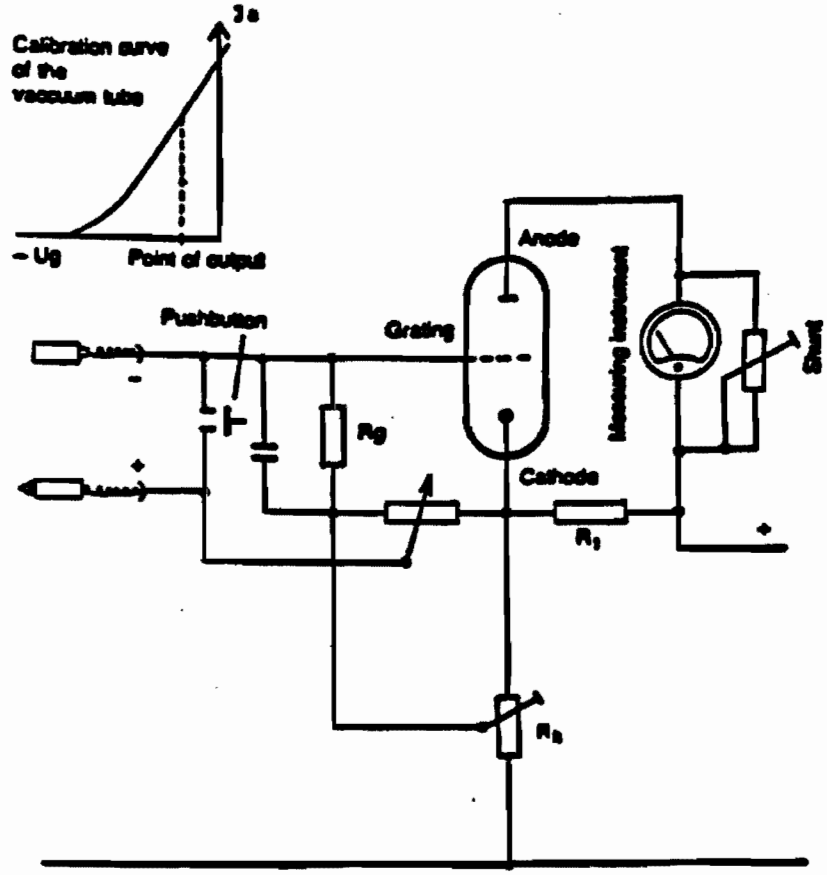

(a)

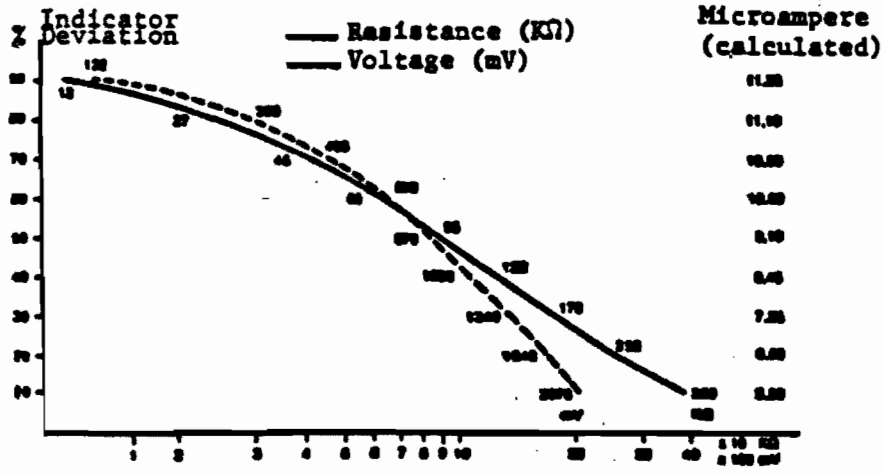

(b)

11. (a) Diagram of connections for the diagnostic part of the K+F-Diatherapuncteur apparatus.

(b) Calibration curve for the above apparatus.

reduces the net resistance of the loop causing the grid bias to become less negative so that the cathode-anode current increases and is registered on the meter (see the calibration curve of Fig. 11). (3) The smaller is the skin resistance, the lower will be the equivalent resistance of the cathode-grid circuit so the more positive will be the grid bias and the larger will be the anode current registered on the meter. Thus, the meter responds in proportion to the skin conductance so it is essentially a conductance meter. (4) The more positive is the grid bias, the greater will be the current flowing in the cathode-grid circuit, a part of which also flows through the skin resistor in such a way as to make the sylis-electrode have a positive potential relative to the hand-electrode. (5) This anodic potential applied to the skin causes ion flow through the skin in such a direction as to increase the skin resistance (see Fig. 3) and sets in motion a change in grid-bias such that the cathode-anode current in the tube decreases and an indicator drop (I.D.) occurs on the meter.

It is also important to note that the effective skin resistance depends upon the pressure applied to the stylis electrode and the angle at which it is applied to the skin. In all cases, the stylis should be applied almost perpendicular to the skin to obtain a constant electrode contact area. As the axial force on the contact area is increased, the resistance decreases until a plateau is reached in the range of 0.6--1.6 Kg. Using a constant pressure electrode, when the spring pressure was such as to fall in this range, the normal value of the indicator meter (50 scale units) was registered for healthy subjects.

APPENDIX B

Dielectric Response in Human Skin

A. Complex Electrical Quantities

To characterize the skin as an electric network means that both resistive (ΣR_i) and capacitative (ΣC_i) parameters must be measured. This eliminates any reliance on d.c. measurements (purely resistive) and greatly limits the usefulness of time-dependent or single relaxation-time determinations, as will be shown later.

The most straightforward expressions of useful electrical quantities are as complex numbers in the frequency domain. A valuable technique for the representation of these quantities is to plot the real versus the imaginary parts of the quantity at various frequencies. The frequency dispersion of these values then produces geometric loci of points which are combinations of, or variations on, semicircles and vertical lines. These shapes allow for extrapolation to critical frequency ranges at which actual property values for particular network components can be obtained. As an example, consider Figs. 19a and b, where two simple networks are shown along with their corresponding plots of imaginary (X) versus real (R) impedance components.

Figures 19c and d illustrate the effects of adding one more parameter to the circuit. Note that in Fig. 19c, the R_1-C_1 and R_1-C_2 relaxation times are sufficiently different that the semicircle and straight line are distinct. However, if C_1 and C_2 are similar (say within two orders of magnitude), the shapes will

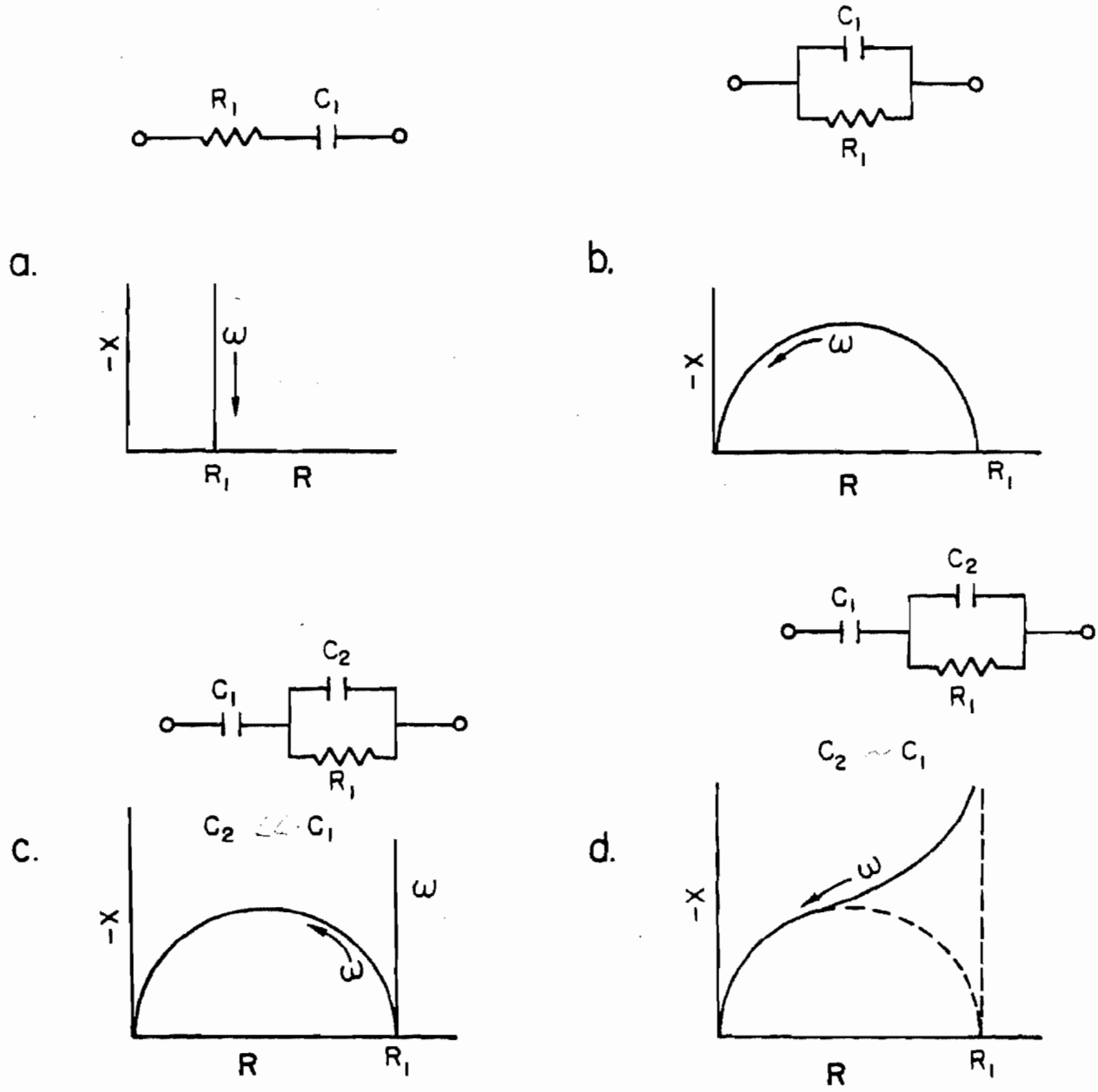

19. Complex impedance plots for (a) series R-C circuit, (b) parallel R-C circuit, (c) $C_2 \ll C_1$, (d) $C_2 \sim C_1$.

overlap. The analysis of Fig. 19d, then, consists of separating out contributions to the curve shape which correspond to a particular relaxation time or R-C combination.

The complexity of any real system makes this a difficult problem which is compounded by the limitation of the experimentally available frequency range. Often not realized, however, is the considerable complementary information obtained by converting impedance values to those of other electrical quantities such as admittance and permittivity (complex dielectric constant). Since admittance is the reciprocal of impedance, a series R-C combination now plots as a sermicircle in the complex plane while a parallel combination gives a straight line. The permittivity plot offers the advantage of extrapolating to values of dielectric constant on the abscissa. Equations B1-B7 show the simple relations between these quantities.

$$Z^* = \text{impedance} = R - jX \tag{B-1}$$

$$Y^* = \text{admittance} = G + jB \tag{B-2}$$

$$\epsilon^* = \text{permittivity} = \epsilon' - j\epsilon'' \tag{B-3}$$

$$G = \text{conductance} = R/(R^2 + X^2) \tag{B-4}$$

$$B = \text{susceptance} = X/(R^2 + X^2) \tag{B-5}$$

$$\epsilon' = \text{dielectric constant} = B/\omega\epsilon_0 \tag{B-6}$$

$$\epsilon'' = \text{dielectric loss} = G/\omega\epsilon_0 \qquad \text{(B-7)}$$

where R is resistance, X is reactance, ω is the radial frequency and ϵ_0 is the permittivity of free space. It will also be seen that, over a given frequency range, one plot may prove much more valuable than another for the purpose of extrapolation.

If all the components of a real equivalent circuit were discrete frequency-independent parameters, the analysis would be relatively straightforward. This, however, is never the case and considerable controversy has been generated over apparently frequency-dependent resistances and capacitances which cause complex plane semicircles to appear to be centered below the real axis and straight lines to be inclined from the vertical.

B. The Electrode Problem

Warburg (40) first considered the electrical response of the interface between a metal electrode and a liquid electrolyte. He found that, at a single frequency, the reactance and the resistance are equal and that, over a limited frequency range, the values of both X and R vary inversely as the square root of the frequency. Although Fricke (41) showed that this is only approximately true, it is still generally accepted as Warburg's law that $X \approx R$ and that each varies as $\sim \omega^{-\alpha}$ where α is near 0.5.

The Warburg behavior can be caused by a faradaic process in which current crosses the interface by means of an electrochemical reaction. This is in contrast to a non-faradaic process in which charged particles do not cross the interface but instead

charge and discharge the electrical double layer.

Grahame (42) states as three examples of faradaic processes: (a) a product of electrolysis diffusing away from the reaction site, (b) a reaction product undergoing a second reaction which calls for continuous replacement, and (c) a reaction product reaching an upper limit of chemical potential before the counter electromotive force needed to stop the reaction is attained. These examples all have in common the effect that the electrode is incompletely blocking to species of the electrolyte. An important point is that, since the electrode may be blocking to some species and not to others, a double layer capacitance may and usually does occur in parallel with a faradaic or diffusional admittance. MacDonald (43) has given this behavior a rigorous theoretical treatment.

The application of the diffusional admittance concept to biological systems is obvious since, in an electrodermal measurement, a metal electrode will be in contact with a sodium chloride solution (sweat). However, there is no fundamental reason why the faradaic process should be limited to metal-liquid systems, and one might envision the highly resistive stratum corneum as a semi-blocking electrode in contact with the less resistive deeper-lying tissues.

In characterizing the behavior of several interface situations, Grahame suggested that an Ag/AgCl electrode in contact with an alkali halide solution might not exhibit a faradaic current since the activity of the AgCl is practically invariant. Investigations by Geddes (44) and by Nagel and Tiller (5) have verified

this by showing that the electrical response of Ag/AgCl electrodes, when used with a sweat-simulating solution such as Beckman Paste, is virtually frequency-independent. Under these conditions, any diffusional process in an electrodermal measurement must originate in the body itself. As we shall see, this is the case, and the question is raised whether Warburg-like behavior actually requires an electrochemical reaction process or whether such a mechanism is only one explanation. In fact, this behavior is indicated whenever the current flow is diffusion limited rather than activation limited. Further investigations may find that seemingly unrelated phenomena, such as the selective permeability of biological membranes or simultaneous electronic and ionic currents, will also produce this effect.

C. The Search for an Equivalent Circuit

References to the many aspects of electrodermal measurements can be found in reviews by Edelberg (45), Venables and Martin (46) and Schwan (47). A considerable amount of information is presented by Cole (48) who has rather subjectively traced the development of electrical measurements on membranes.

Fricke (41) and Cole (49) first treated the problem of anomalous frequency dependences in cell suspensions and tissues. Complex plane plots of impedance at high frequencies showed semicircles which were lowered below the bascissa by less than the forty-five degrees predicted by Warburg's law; i.e., $\alpha < 0.5$. Results were reported for each system in terms of a constant phase angle where

$$\theta = \alpha\pi/2 \qquad \text{(B-8)}$$

Although recognizing the similarity to Warburg's electrode polarization behavior, Cole believed that the marked deviation of from 0.5 might require an alternative explanation. Cole and Cole (50) then derived an expression which described their data in terms of the observed phase angle for each system. They assumed a distribution of relaxation times (τ = RC) which would cause a broadening of the frequency dispersion and could result from geometric or cellular inhomogeneities within the sample. Schwan (51) contrasted the Cole-Cole type distribution to that of a statistical distribution of τ and later (Schwan 52) proposed ways of determining whether polarization or some other factor is responsible for the frequency-dependent reactance. Cole (49) proposed the circuit of Fig. 20a to describe his results where R_b, the bulk resistance, is in series with Z_p, a frequency dependent admittance, and R_p, the polarization resistance. Although the Cole-Cole equation has been used by Yokota (53), Yamamoto (54) and many others to fit impedance and permittivity data, it remains only a mathematical description which as yet defies physical understanding.

Barnett (55) dealt with the inconsistent results obtained for the phase angle of human skin in an attempt to separate the skin impedance from that of the deeper-lying tissues. Although his experimental approach was unconvincing, he successfully pointed out that more than one phenomenon may be superimposed in a

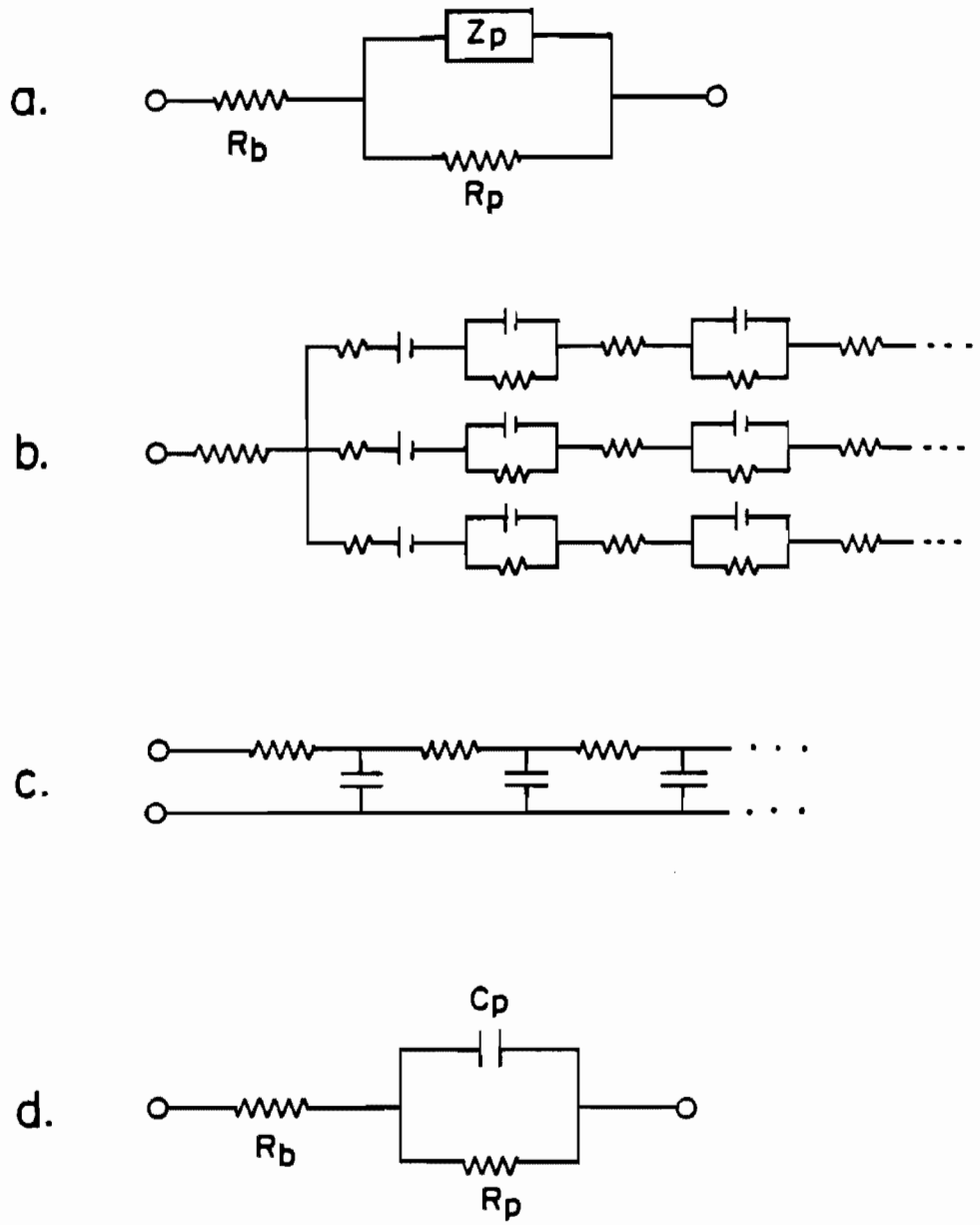

20. (a) Equivalent circuit described by the Cole-Cole equation.
(b) Circuit describing laminated structure of skin according to Tregear (56).
(c) Equivalent circuit of transmission line described by Warburg's law.
(d) Frequency-independent circuit assumed in analog pulse techniques.

single set of measurements. Tregear (56) suggested that the electrodermal response be broken down into contributions from each skin layer, as in Fig. 20b. Although this circuit does predict a frequency dependence, it is hardly experimentally confirmable and one might consider whether such a nearly infinite array of circuit elements might be lumped into one frequency-dependent element. It should be noted that the Warburg admittance itself is described by the infinite transmission line network of Fig. 20c.

More recent attempts to separate out the effects of the stratum corneum from those of the deeper tissues have been performed by Yamamoto (57), Lawler, et al. (58), and Lykken (2), through the stripping off of successive layers of skin. This work indicates that nearly all of the resistance is in the epidermal layer, which might allow one to consider anything below this layer as deep tissue.

D. The Speed for Accuracy Trade-off

The measurement of impedance was made possible by modification of the Wheatstone bridge to operate over a range of frequencies. And still, the comparison of the sample-electrode system to a set of variable capacitors and resistors is the most accurate method for determining impedance. However, there are two major drawbacks to the use of a bridge circuit in measuring frequency response. One is the limited frequency range over which it is reliable. The other is the time required for taking readings at a sufficient number of frequencies. For bridge readings to be self-consistent, one must assume the sample to be in equilibrium,

and, in skin measurements, this cannot be assumed until at least thirty minutes after the application of electrodes.

Lykken (2) has proposed the use of square wave analysis in which a step voltage is imposed across the sample and the current is monitored to give values of resistance both before and after the charging of the capacitative elements. This method provides an effective way of covering a wide frequency range in a matter of seconds, but it also has several drawbacks. First, the initial or peak current value is dependent on the rise times of both the generator and the measuring device (usually an oscilloscope). Indeed, analog measurements have limited accuracy over such short decay times. Second, and most serious, is that only one relaxation time can be monitored, and one must assume a network where the polarization reactance of Fig. 20a becomes a simple double layer capacitance (Fig. 20d).

A steady-state method, which provides an improvement over both the precision and accuracy of analog pulsed measurements, is reported in the Bode plot analysis of Burton, et al. (59). This procedure permits the synthesis of an equivalent circuit for any passive system through its frequency behavior. Once that circuit is assumed, measurements need only be taken at three or four critical frequencies to obtain values for the components. The circuit that is generated, however, is not unique and may have no bearing on the physical processes of the system. It also precludes the analysis of frequency-dependent components, which is undoubtedly an oversimplification.

Teorell (60) was able to account for the frequency-

dependent reactance of Fig. 20a using a graphical Fourier analysis to convert data from the time domain to the frequency domain. Although a laborious procedure, it does allow data to be taken quickly. However, it applies only to the frequency range in which the phase angle is constant.

The recent advances in Fourier analysis, notably that of the fast Fourier transform, may ultimately lead to a replacement for the cumbersome bridge technique. There is already a considerable literature relating the application of this method to electrochemical (Sandifer and Buck (61)) and biomedical (Yoganathan, et al. (62)) research. For our purposes, however, its usefulness seems to be contingent on the adequate refinement of an equivalent circuit for the skin. In the following section, Nagel and Tiller (5) report on preliminary attempts from this laboratory to provide such a circuit from which meaningful component values may be extracted.

E. An Analysis of Complex Plane Plots

A comparison bridge circuit was modified to operate in the frequency range from less than 10 Hz to more than 100 kHz. Bridge balance was detected by a low-level differential oscilloscope.

Beckman Ag/AgCl electrodes (.01 m diameter) were attached to the volar forearm of each subject. The electrode spacing was 0.12 m. The subjects, all adult volunteers, were asked to relax in a reclining position inside a Faraday cage. Impedance data were taken at various frequencies during the first thirty minutes and were time-dependent. Once the readings stabilized, a series

of about 40 readings was taken at frequencies from 40 Hz to 100 kHz. Voltage across the system was maintained at 0.4 V. The data was either in the form of series capacitance vs. dissipation factor or of parallel capacitance vs. quality factor. A small computer was used to convert these data to complex impedance, admittance and permittivity.

If an appropriate equivalent circuit were known, values for the components of the circuit could be readily obtained through iterative curve fitting. Since this is not the case, we must search the data for clues that will suggest certain component configurations and eliminate others. The following paragraphs briefly illustrate the use of a complex plane analysis for examining data from the human body.

Figure 21 shows typical complex plane plots obtained in this laboratory. The depressed impedance semicircle (Fig. 21a) seems well described by the Cole circuit (Fig. 20a), and one is tempted to extrapolate to a high frequency value of R_b and a low frequency value of $R_b + R_p$, where R_p is now the resistance of the stratum corneum. The complex admittance (Fig. 21b) seems also to support this circuit with the extra advantage of allowing a more accurate extrapolation to low frequency. However, the complex permittivity, or Cole-Cole plot (Fig. 21c), which is often ignored in these treatments, indicates a completely different interpretation.

In Fig. 21c, there is additional information at high frequency that is masked in the previous figures. If we extrapolate the high frequency arc as a semicircle, we see that it is

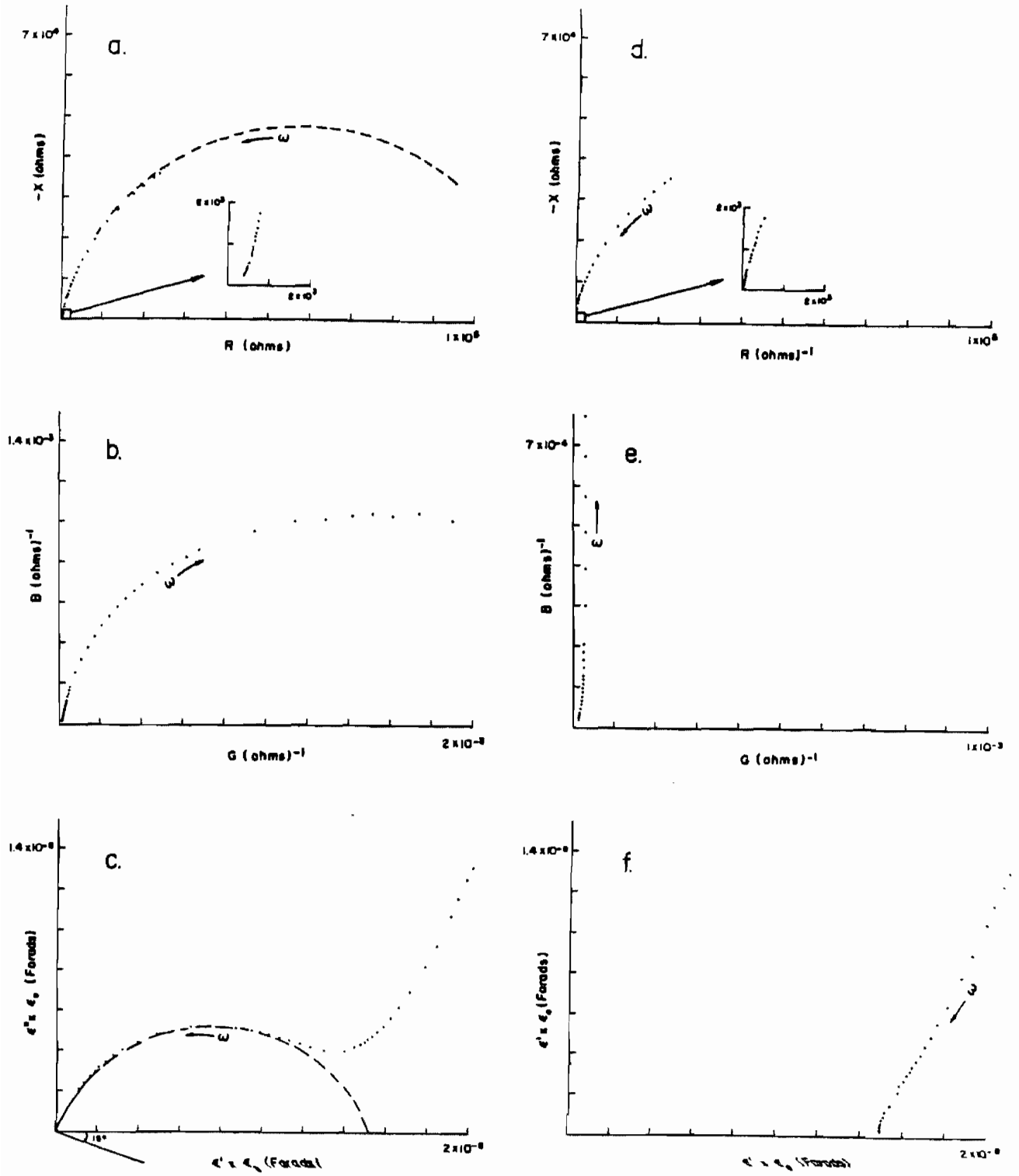

21. (a,b,c) Complex plane representation of electrical response at volar forearm of human subject: impedance, Z^*; admittance, Y^*; permittivity, ϵ^*. (d,e,f) Complex plane representation of a, b and c after subtracting assumed high frequency (deep-tissue) contribution.

lowered below the axis by about 19° and that its low frequency intercept corresponds to an apparent capacitance of ~ 1.4 x 10^{-8}F. Similar values have been assumed for the double layer capacitance of the skin. The lowering of the semicircle is consistent with a high frequency diffusional admitance (Z_I) of the general form.

$$Y^*_{Z_I} = A_1 \omega^{\alpha_1} + j A_2 \omega^{\alpha_2} \qquad \text{(B-9)}$$

in series with the apparent low frequency capacitance. Implicit in this expression is that θ of eq. B-8 is the angle by which the semicircle is lowered. As a first approximation, then, we have isolated both a high and a low frequency component from the total circuit (Fig. 22a). Note that this combination is inconsistent with any portion of the previously proposed circuits.

If Z_I does describe the high frequency regime, then we can subtract the assumed double layer capacitance directly from the impedance data of this region and a replotting in the permittivity plane should give a curve shape corresponding to Z_I alone. This manipulation replaces the semicircle of Fig. 21c by a line inclined from the vertical which is straight within the limits to which the capacitance value can be estimated. The straight line can now be analyzed by converting eq. B-9 to an expression of permittivity.

$$\epsilon_0 \epsilon^*_{Z_I} = A_2 \omega^{(\alpha_2 - 1)} - j A_1 \omega^{(\alpha_1 - 1)} \qquad \text{(B-10)}$$

By writing the real part of the permittivity as

$$\ln \epsilon' = \ln A_2 + (\alpha_2 - 1) \ln \omega \qquad \text{(b-11)}$$

and similarly for the imaginary part, the parameters A_1, A_2, α_1 and α_2 can be evaluated through a first order polynomial regression. The values of these parameters for the present set of data are listed in Table 1. Note that $\alpha_1 \approx \alpha_2 = 2\theta/\pi$ and that $\theta \approx \tan^{-1} (A_2/A_1)$.

To check whether Z_I adequately characterizes the high frequency response, we can subtract it from the original impedance data and begin the analysis again as though the component were not present. Figure 21f shows that the high frequency semicircle is now removed from the permittivity plot but that the low frequency range is relatively unaffected. The equivalent effect is seen in the admittance plot where the high frequency portion is a straight line, but the low frequency region remains inclined (Fig. 21e). The new impedance curve of Fig. 21d, however, has only been shifted to the origin at high frequency. This very important observation shows that the assumption of extrapolating the impedance data to a high frequency fixed resistance value is erroneous. In other words, Fig. 21a may not continue to a finite point on the abscissa, but may slowly go to zero with increasing frequency. What one is seeing in Fig. 21a, then, is the effect of the polarization reactance as it overrides Z_I and brings the data into an experimentally observable range. This also means that, in the pulse or square wave techniques, the initial current value does not correspond to a fixed bulk resistance but instead is a function of the

rise time (effective upper frequency limit) of the measuring system.

The high frequency portion of the equivalent circuit can now be modified for electrochemical consistency, as in Fig. 22b, where C_g is the geometric or optical capacitance corresponding to the infinite frequency dielectric constant (ϵ_∞). The value for this capacitance is expected to be low (10^{-12} - 10^{-11} F), and its effect on data beow 50 kHz should be negligible. R_1 functions as the faradaic admittance which necessarily shunts Z_I. Further experimentation should determine whether R_1 denotes a bulk resistance or whether it is a parameter dependent on the values assigned to Z_I.

This model assumes that all high frequency phenomena correspond to the bulk or deeper-lying tissues of the skin and that they will act in series with any polarization, epidermal or electrode effects. We can now evaluate the low frequency behavior from Fig. 21 since it appears that the major high frequency contribution has been successfully subtracted out of the data. Figure 21f indicates that a fixed double layer capacitance does exist and is in parallel with a large resistance which is undoubtedly that of the stratum corneum. From the admittance plot of Fig. 21e, this resistance value can be estimated. The lowered semicircle of Fig. 21d, however, indicates that a frequency-dependent parameter is still present and adding a Warburg-like behavior to the circuit. According to Grahame (42), this component can be considered in parallel with the double layer capacitance and, if so, the low frequency circuit might be represented

as in Fig. 22c. Reasonable values for C_{dl} and R_2 can now be subtracted from the remaining admittance and the result for all three plots is a straight line with a slope from the vertical corresponding to Z_{II}. This can be analyzed by polynomial regression of the logarithm of eq. B-9 to give approximate values for its frequency dependence and coefficients. These estimates are shown in Table 1.

At this stage, the approximations become decreasingly valid because of the complex interactions between parameters. For example, the reactance of Z_{II} is of the same order as that of C_{dl} and the influence of Z_I on the low frequency region will depend upon the frequency at which it is shunted by R_1. Undoubtedly, there are other minor contributions to the circuit which haven't been considered, and the configuration may not be unique or even correct in spite of its response to physical interpretation.

An iterative curve-fitting computer program has successfully eliminated several other circuit configurations and is now being used in an attempt to best fit the present twelve parameters of Fig. 22d to the data. However, more advanced instrumentation and, particularly, a wider frequency range may be required before further understanding can be obtained.

Although this discussion is necessarily incomplete, there are several observations to be made at this point. The diffusional admittance appears to be a more general concept than has previously been recognized. In this system, two such admittances have been isolated, and neither seems related to Warburg's original treatment of polarization at metallic electrodes. Indeed,

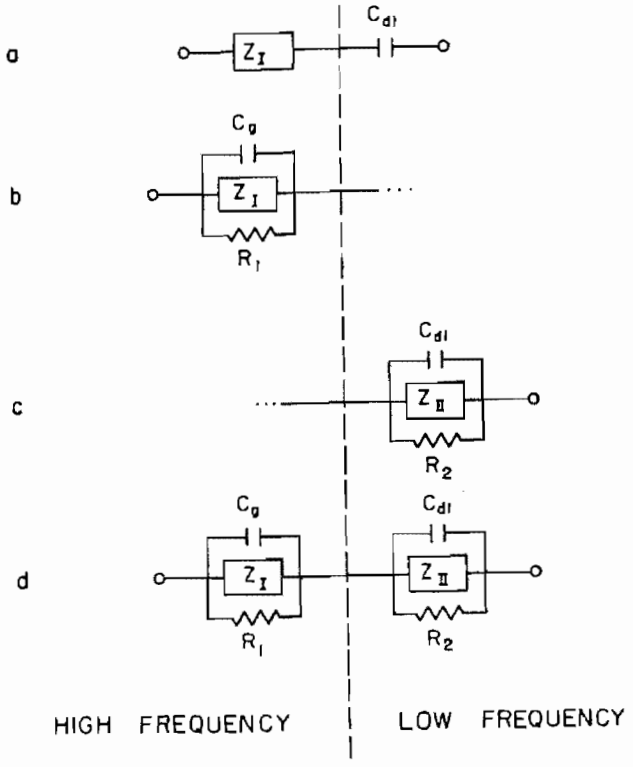

22. Sequence of equivalent circuit generated by complex plane analysis described in text.

Table 1

Estimates of parameters in the diffusional admittances of Figure 21d.

$$Y_Z^* = A_1\omega^{\alpha_1} + jA_2\omega^{\alpha_2}$$

	$Z=Z_I$	$Z=Z_{II}$
α_1	0.18	0.54
α_2	0.18	0.54
A_1 (mho)	1.8×10^{-4}	1.4×10^{-7}
A_2 (mho)	6.4×10^{-5}	1.7×10^{-7}

should metal electrodes have been used, one might expect that additional polarization complexities would have been encountered. Contributing mechanisims have only tentatively been assigned to this behavior.

Other conclusions from this work are more straightforward. The limitations of pulsed techniques which rely on a three-component equivalent circuit become obvious. The fallacy that frequency-dependent bridge measurements can be extrapolated to values of resistance or capacitance without appropriately considering diffusional admittances has also been pointed out. If the electrical properties of the skin are to be elucidated, and, indeed, if changes in these properties monitor changes in body functions, then further investigations based on an adequate equivalent circuit are called for.